

Chapter 13

Simulink Tutorial on Digital Modulation Methods

13.1 Preview

This chapter is the guideline for a software tutorial on selected problems of frequency carrier modulation methods covered in the previous chapters. The programs are written in Simulink and Matlab. By kind permission from MathWorks, the software package contains some functions and blocks from Matlab toolboxes and Simulink blocksets which are not included in the standard student version of Matlab and Simulink. This allows the student to run the tutorial with the standard student version of Matlab and Simulink under Windows and Linux. These functions and blocks are not supported by MathWorks. For other platforms than Windows and Linux you will need the *Signal Processing Toolbox* as well as the *Communications Toolbox*, the *Communications Blocksets*, and the *DSP Blocksets* in addition to the standard Matlab/Simulink student version.

The goal of this tutorial is to illustrate digital modulation methods that were previously presented theoretically and to achieve a better understanding by observing and experimenting with some parameters. Additional theory is provided where needed. Some theory is sometimes extended, providing a different view on the problems. According to the tutorial character of this chapter, we do not simply present the material but formulate problems that enable more active study whereby students can check their level of understanding. The sections are organized into a theory part including problems and a practical part describing experiments using the Simulink programs.

Since many students may be less familiar with Simulink than with Matlab, we first give a short introduction to Simulink in Section 13.2. The tutorial is based on a transmission scheme as depicted in Figure 7.20 and covers pulse shaping (13.4), BPSK (13.5), QPSK (13.6), Offset-QPSK (13.7) and 16-QAM (13.9). In Section 13.8 we describe an offset-QPSK representation of binary orthogonal frequency-shift keying (minimum shift keying (MSK)) which shows that MSK can also be viewed as a linear

modulation method. The software package also includes tutorials on on-off keying and 4-ASK. To start the tutorial, go to the directory where you saved the tutorial files and type *DigModTutorial* in the Matlab workspace. The main menu depicted in Figure 13.13 will open from which you can choose the parts of the tutorial.

13.2 Short Introduction to Simulink

In this section we give a short introduction to Simulink using BPSK transmission as an example. However, we restrict ourselves to the principles of Simulink and the features needed in the tutorial. For more detailed information, we refer the reader to the Simulink manual. Figures are printed as they appear under Windows. They may appear slightly different under Linux.

Simulink is a program for simulation of dynamic systems that provides a graphical interface. Within the Matlab environment it is a toolbox. Dynamical systems are often represented using block diagrams. The graphical interface allows us to use such a block diagram directly for programming Simulink. The dynamical system in our case is the digital modulation scheme with time-varying data.

Simulink is started by the command

```
simulink
```

from the Matlab workspace. The *Block Library Browser* will open and provide the blocks available in the Simulink library (see Figure 13.1).

The library is subdivided according to the functions of the blocks, such as *Sources* or *Sinks*. You can open a library by double-clicking on the respective button.

13.2.1 Example: BPSK Transmission

We use BPSK transmission with rectangular pulses to demonstrate how to use Simulink. The goal is to build the Simulink model depicted in Figure 13.2.

In order to build a new Simulink model, open a new model from the menu

```
File > New > Model
```

A library block can simply be dragged from the library window to the Simulink model window.

We used the *Uniform Random Number Generator* followed by the *Sign* block as a binary source in Figure 13.2. The *Uniform Random Number* block generates uniformly distributed random numbers over a specified interval. In our example the random numbers are drawn from the interval $[-1, +1]$. The output of the subsequent *Sign* block is 1 when the input is greater than 0, 0 if the input is 0, and -1 when the input is less than 0. In order to generate a binary source that outputs the bits +1 and -1 with equal probability, we add a *Look-Up Table* block, which maps the input +1 to +1, -1 to -1, and 0 to +1. To add the *Uniform Random Number* block to your model, double-click on *Sources* in the Simulink Block Library Browser. This will display the *Sources* library

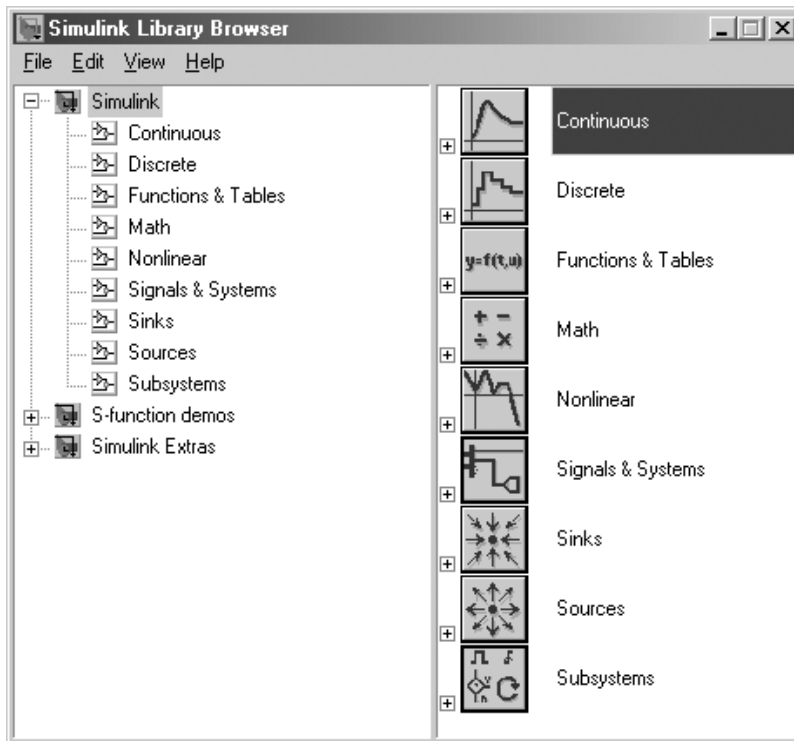


Figure 13.1: Simulink Block Library Browser

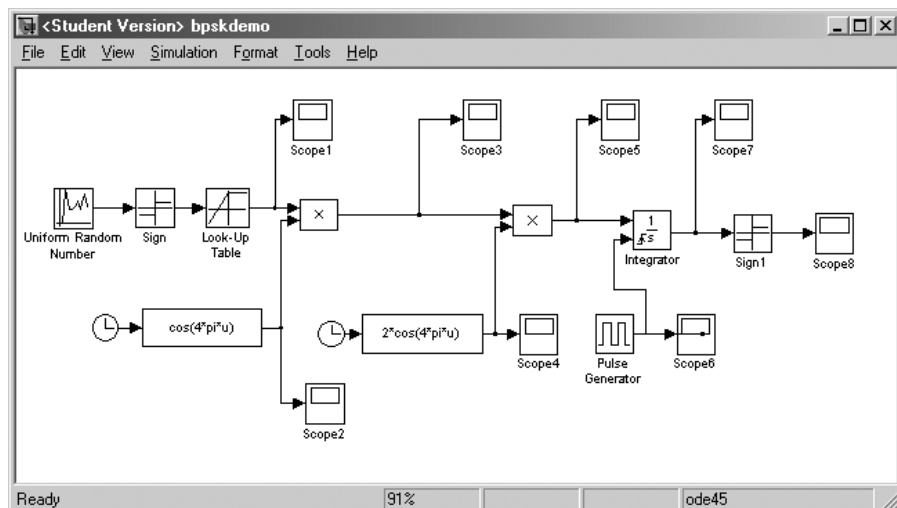


Figure 13.2: Simulink model for BPSK transmission

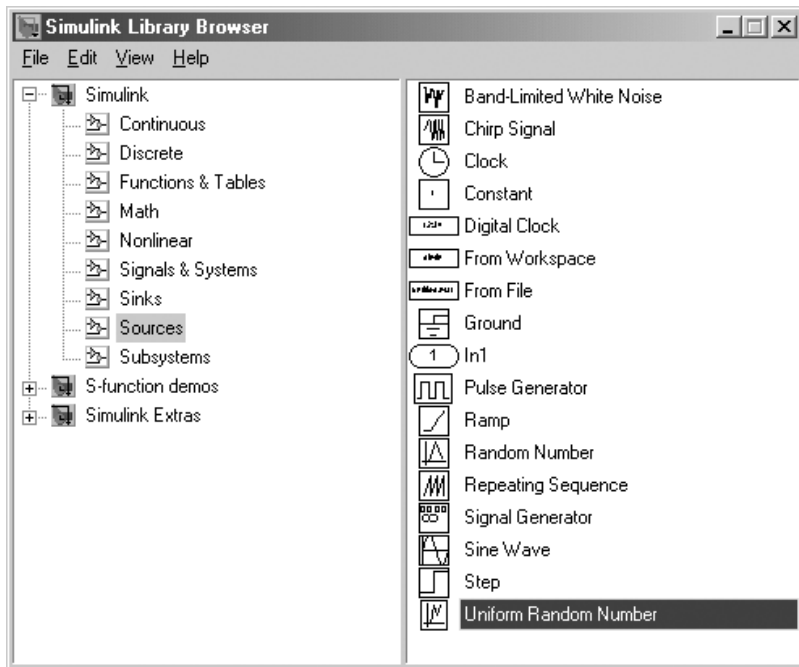


Figure 13.3: Sources library

(see Figure 13.3). Drag the block *Uniform Random Number* to your Simulink model and double-click on it.

This will open the *Block Parameters* window as depicted in Figure 13.4, where you can input the parameters as given in Figure 13.4. Now, drag the *Sign* block from the *Math* library to your model. Connect the blocks *Uniform Random Number* and *Sign* using the mouse: Press the left mouse button on the *Uniform Random Number* block output and drag the mouse pointer to the input of the *Sign* block. Release the mouse button. The *Look-Up Table* block is taken from the *Functions & Tables* library. Double-click on the *Look-Up Table* block in your model and input the block parameters as given in Figure 13.5.

The signals at any point of the system can be viewed using the block *Scope* from the *Sinks* library. Connect a scope to the output of the block *Look-Up Table*.

Before we can start the simulation to view the source signal we have to adjust the *Simulation Parameters*. The *Simulation Parameters* window depicted in Figure 13.6 is opened with the command

Simulation > Simulation parameters

from the menu bar. For now, only the parameters *Start time* and *End time* are relevant. Later you may need to adjust *Max step size* and *Min step size* for numerical integration

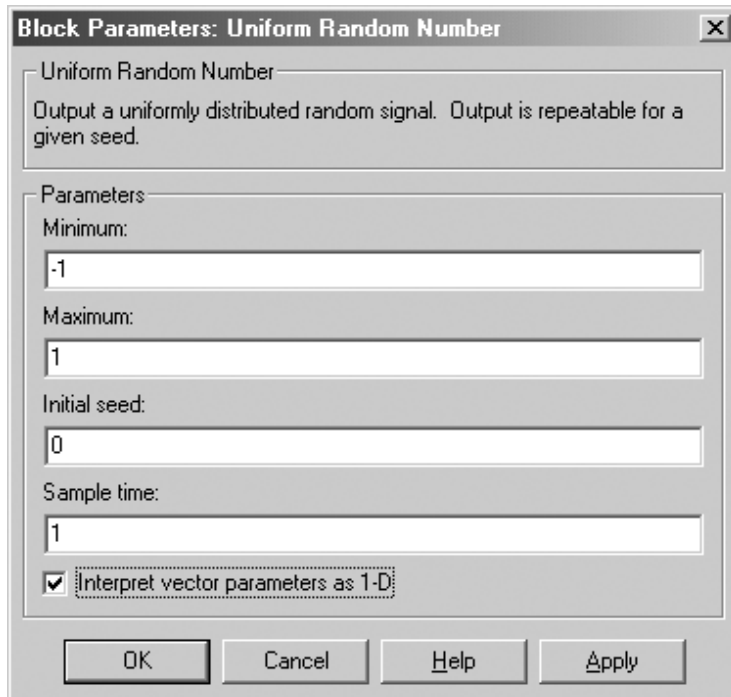


Figure 13.4: Block parameters: Uniform Random Number

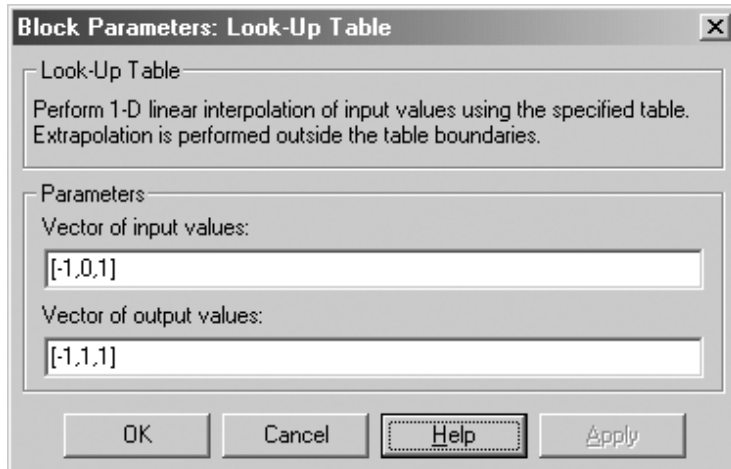


Figure 13.5: Block parameters: Look-Up Table

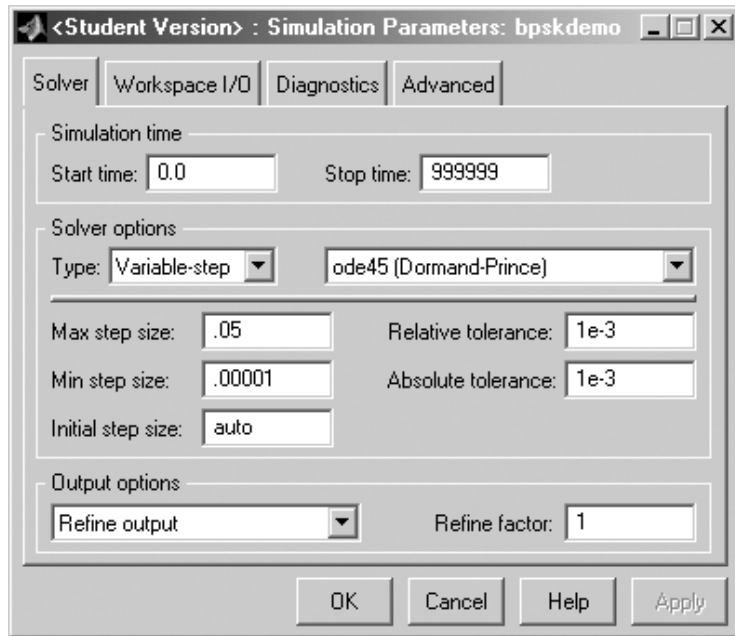


Figure 13.6: Simulation parameters window

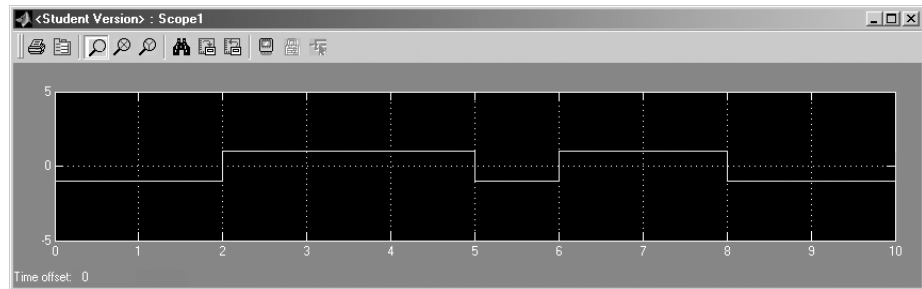


Figure 13.7: Source signal (Scope1)

in order to obtain accurate results. The simulation is started from the menu bar with the command

Simulation > Start

Similarly, the simulation is stopped using

Simulation > Stop

To view the source signal, a double-click on the scope will open a window as depicted in Figure 13.7.

A right mouse-click on the window opens a pop-up menu from which you can open the *Axes properties* window, depicted in Figure 13.8, in order to set the range of the y axis.

The time range of the *Scope* window can be changed from the *Parameters* button in the menu bar in Figure 13.7 (see Figure 13.9).

The other blocks in Figure 13.2 can be included in the same way. The carrier $\cos(4 * \pi * u)$ is generated using the block *Fcn* from the *Functions & Tables* library. This block applies a specified expression such as $\cos(u)$ to the input variable u . Drag the block *Fcn* to your model and double-click on it. This will open the *Block Parameters* window, as depicted in Figure 13.10, where you can input the expression $\cos(4 * \pi * u)$.



Figure 13.8: Axes properties window of Scope1

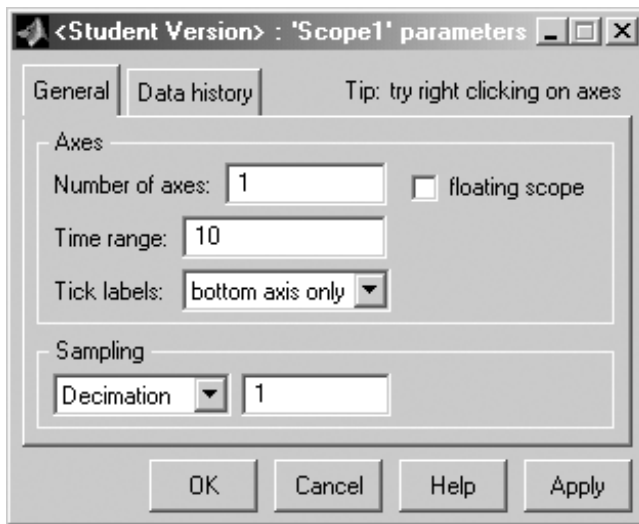


Figure 13.9: Parameters window of Scope1

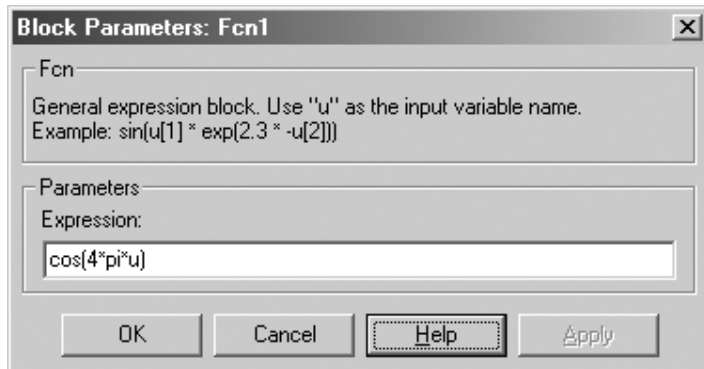


Figure 13.10: Block parameters: Fcn

The time variable u is obtained from the *Clock* block of the *Sources* library. The *Product* block from the *Maths* library is used to generate the modulated signal. We simulate noiseless transmission and therefore just connect the transmitter and the receiver. If you have the *Communications Blockset* available,¹ you can include an AWGN channel between transmitter and receiver. The matched filter at the receiver is realized as integrate and dump using the *Integrator* from the *Continuous* library. The reset signal is generated by the *Pulse Generator* from the *Sources* library with parameters as given in Figure 13.11.

You can get online help on a block from a pop-up menu that is opened by a right mouse-click on the block.

Now, you can start the simulation from the menu bar and view the scope signals at different transmission points. You may need to change the simulation parameters as described in Figure 13.6 to ensure accurate signals.

13.3 Start the Tutorial

In order to run the tutorial add the directory where you saved the files with all subdirectories to your Matlab path. The easiest way to do this is to use the *pathtool*, which is opened by the command

```
pathtool
```

from the Matlab workspace. Click on the button *Add with Subfolders...* as depicted in Figure 13.12 and choose the directory where you saved the tutorial files. The software package contains some functions and blocks from Matlab toolboxes and Simulink blocksets, which allows you to run the tutorial with the standard student version of Matlab and Simulink. These functions and blocks are not supported by MathWorks.

¹The Communications Blockset provides a set of blocks that are often needed for simulation of communications systems. It is not included in the standard Simulink version.

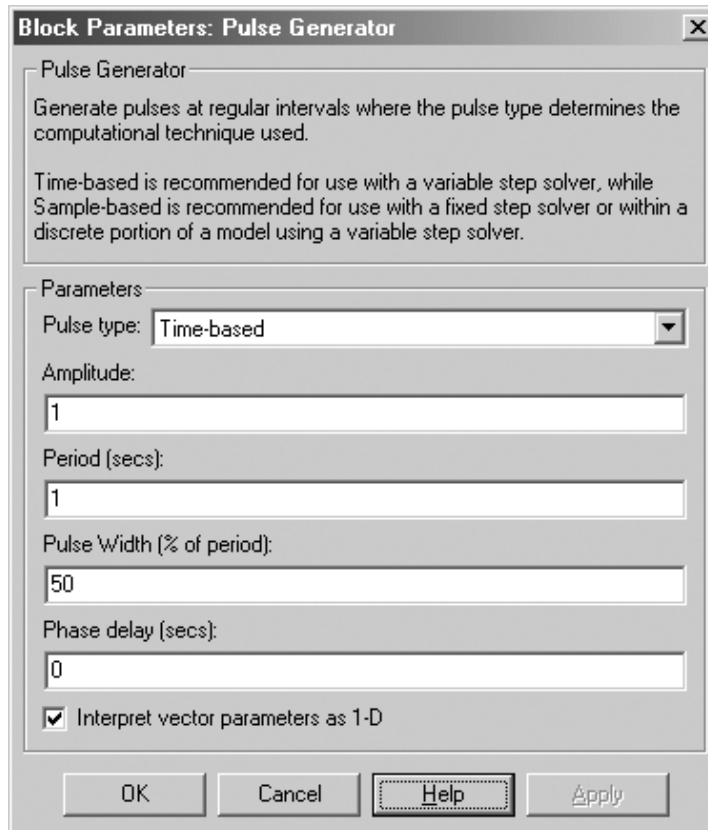


Figure 13.11: Block parameters: Pulse Generators

In order to avoid confusion, we recommend the removal of the directories from your Matlab path if you use Matlab and Simulink with toolboxes for applications other than this tutorial.

To start the tutorial, type

`DigModTutorial`

in the Matlab workspace. The main menu, depicted in Figure 13.13, will open from which you can choose the parts of the tutorial.

13.4 Pulse Shaping

The tutorial covers digital modulation methods with different pulse shaping. The first part presents the pulses and their Fourier spectra. The goal of this part is to illuminate the relevance of pulse shaping for ISI free transmission, which is a basis for the following experiments. This part of the tutorial is written in Matlab.

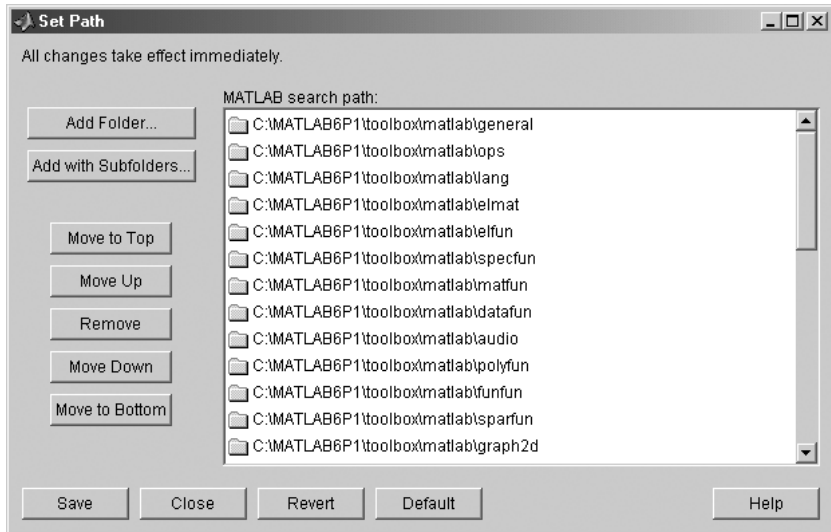


Figure 13.12: Matlab path tool

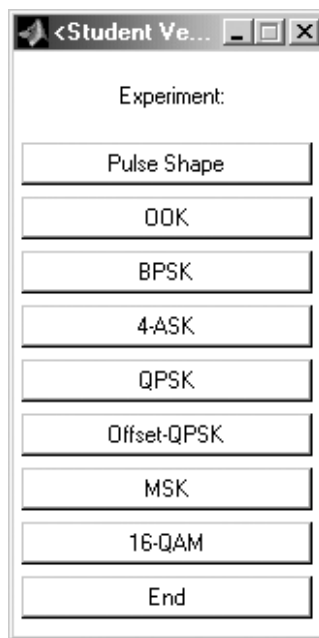


Figure 13.13: Tutorial main menu

13.4.1 Theory

The impulse response $g_T(t)$ of the transmit filter determines the spectral characteristics of the transmitted signal. Impulses that are limited in the time domain are infinite in the frequency domain. On the other hand, bandlimited pulses are infinite in the time domain. Consequently, in order to avoid intersymbol interference (ISI) after sampling, the cascade of the transmit and receive filter

$$g(t) = g_T(t) * g_R(t) \quad (13.4.1)$$

needs to meet the first Nyquist condition, which was discussed in Section 6.5.1.

TUTORIAL PROBLEM

Problem 13.1 [Nyquist Condition (Zero-ISI Condition)] State the first Nyquist condition for zero ISI both for the impulse response $g(t)$ and its Fourier transform $G(f)$.

SOLUTION

$$g(nT) = \begin{cases} 1, & n = 0 \\ 0, & n \neq 0 \end{cases} \quad (13.4.2)$$

$$\sum_{m=-\infty}^{\infty} G\left(f - \frac{m}{T}\right) = T = \text{constant} \quad (13.4.3)$$

In the tutorial we use two types of pulses that meet the zero ISI condition: NRZ (nonreturn to zero) rectangular pulses and raised-cosine pulses (see Section 6.5.1).

TUTORIAL PROBLEM

Problem 13.2 [Eye Pattern] In Section 6.4 the eye pattern was introduced as a method to view the amount of ISI. Try to construct the eye diagram of a raised-cosine pulse with rolloff factor $\alpha = 0$ for binary data. Take into account only the two neighboring interfering pulses. Which bit sequences have to be considered? How does zero ISI show up in the eye diagram?

SOLUTION

Raised-cosine pulse:

$$g(t) = \frac{\sin(\pi t/T)}{\pi t/T} \cdot \frac{\cos(\alpha\pi t/T)}{1 - 4\alpha^2(t/T)^2}$$

The following eight bit sequences have to be considered:

+1	+1	+1
+1	+1	-1
+1	-1	+1
+1	-1	-1

-1	+1	+1
-1	+1	-1
-1	-1	+1
-1	-1	-1

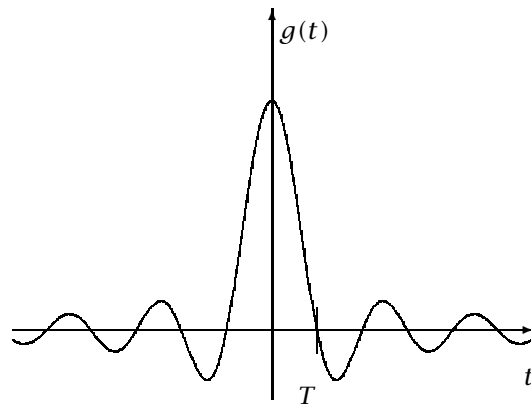
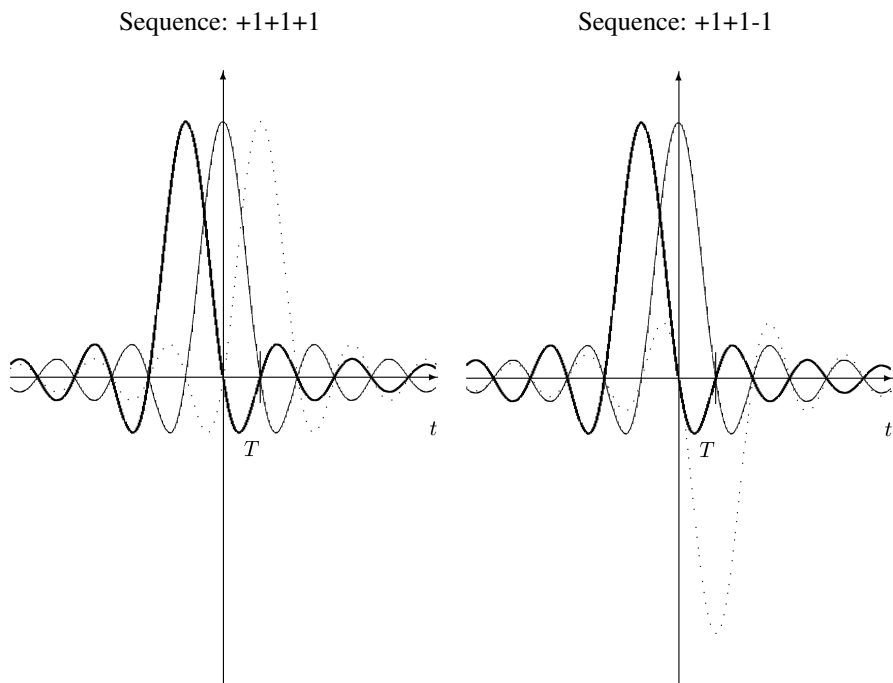
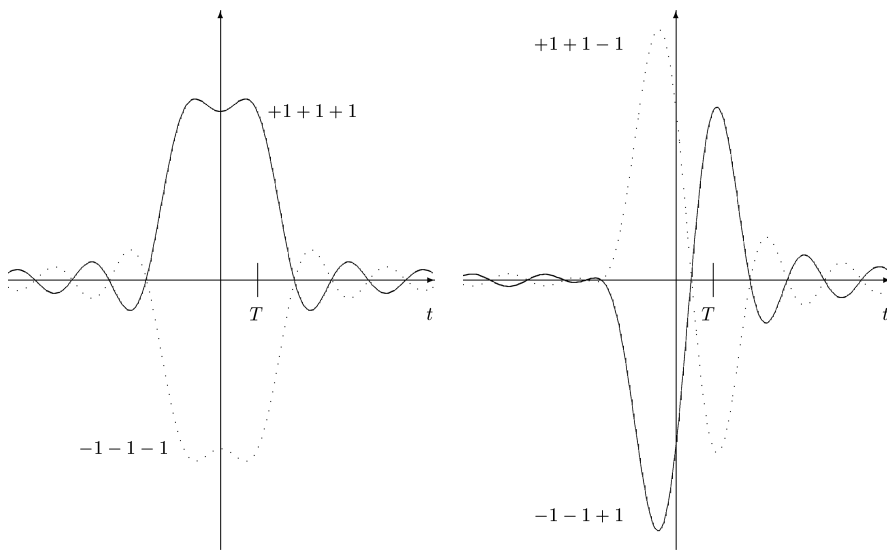


Figure 13.14: Raised-cosine pulse

We construct the eye pattern for the four bit sequences with +1 as center bit (the contributions of the other bit sequences are symmetric):

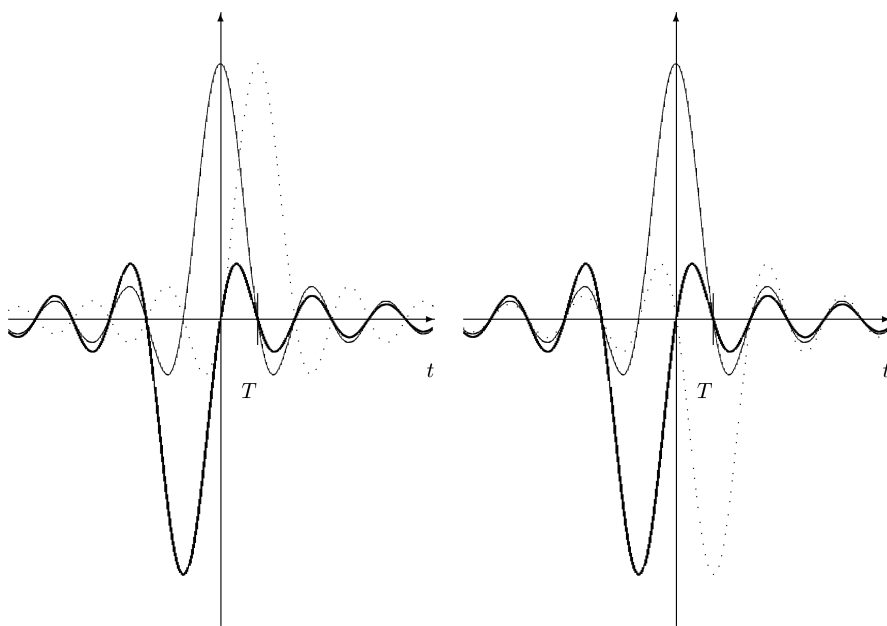


Summation of pulses yields the contribution to the eye pattern:

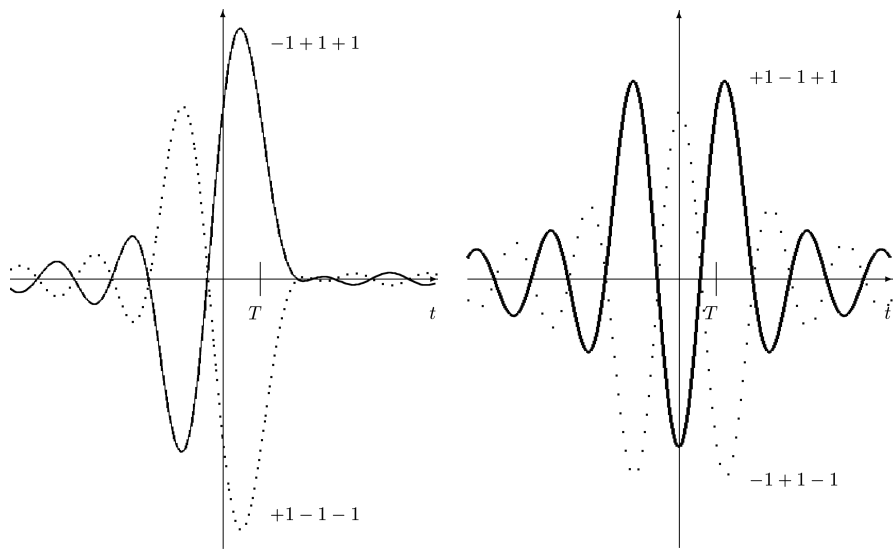


Sequence: $-1+1+1$

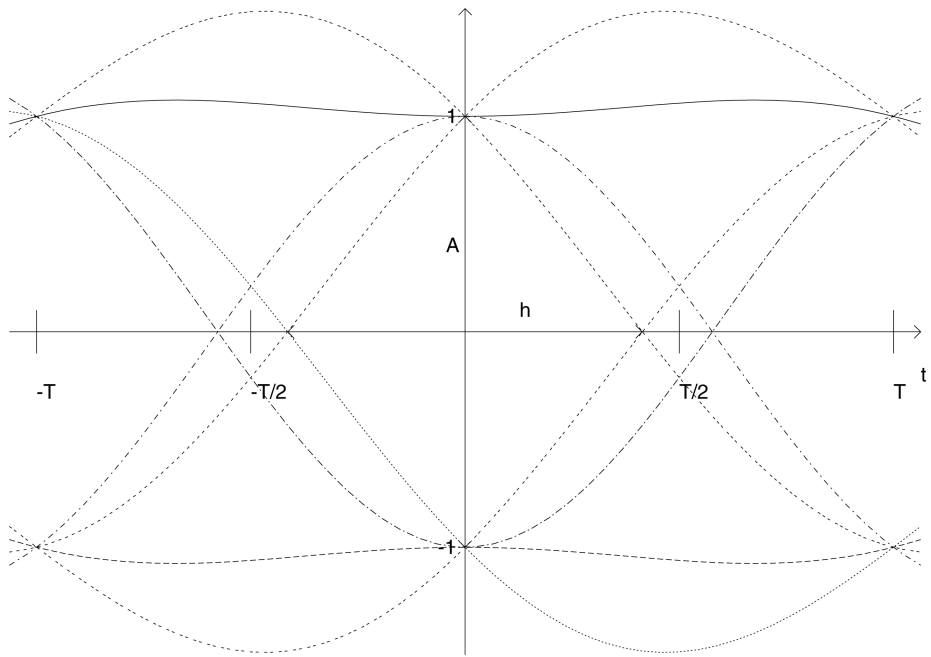
Sequence: $-1+1-1$



Summation:



The eye pattern is the superposition of the contributions of all bit sequences:



Zero ISI means maximum vertical eye opening, i.e., all lines cross at $+1$ or -1 . In order to reduce the sensitivity to timing error, we also wish a wide horizontal eye opening.

For $\alpha = 0.5$ the horizontal eye opening is less than the maximum possible opening of T .

In AWGN channels the optimum receive filter that maximizes the signal-to-noise ratio (SNR) is the matched filter

$$g_R(t) = g_T(-t) \quad (13.4.4)$$

Consequently, the maximum SNR at the receive filter output is obtained if the Nyquist pulse shaping is split equally between the transmit and receive filter. Therefore, the Fourier transform $G_T(f)$ should have a square-root raised-cosine characteristic (see Illustrative Problem 6.8).

The impulse response and the Fourier transform of a square-root raised-cosine pulse are given by

$$g_T(t) = \frac{(4\alpha t/T) \cos[\pi(1 + \alpha)t/T] + \sin[\pi(1 - \alpha)t/T]}{(\pi t/T)[1 - (4\alpha t/T)^2]} \quad (13.4.5)$$

$$G_T(f) = \begin{cases} \sqrt{T}, & 0 \leq |f| \leq \frac{1-\alpha}{2T} \\ \sqrt{\frac{T}{2} \left[1 + \cos \frac{\pi T}{\alpha} \left(|f| - \frac{1-\alpha}{2T} \right) \right]}, & \frac{1-\alpha}{2T} < |f| \leq \frac{1+\alpha}{2T} \\ 0, & |f| > \frac{1+\alpha}{2T} \end{cases} \quad (13.4.6)$$

If a square-root raised-cosine transmit filter $g_T(t)$ is used, there is zero ISI after the receive filter but ISI results for the transmitted signal.

13.4.2 Experiments

To start the tutorial go to the directory where you saved the tutorial files and type *DigModTutorial* in the Matlab workspace. The main menu depicted in Figure 13.13 will open. Choose *Pulse Shape* from the main menu, then *NRZ Rectangular* in the menu *Pulse Shape* (see Figure 13.15):

Pulse Shape > NRZ Rectangular

The pulse shape and the Fourier spectrum of an NRZ rectangular pulse will be displayed as depicted in Figure 13.16.

TUTORIAL PROBLEM

Problem 13.3 [NRZ Rectangular Pulse]

1. Is the zero ISI condition met ?
2. An NRZ rectangular pulse has a finite-duration impulse response. What does this mean for the bandwidth?

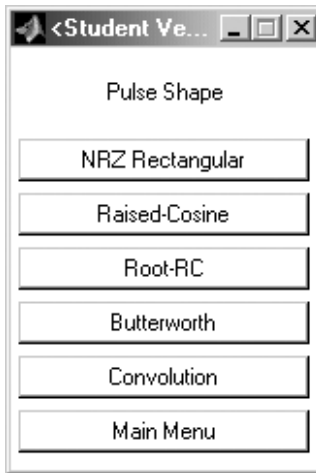


Figure 13.15: Menu for experiment *Pulse Shape*

SOLUTION

1. Yes, because the pulse is limited to T .
 2. A finite-duration impulse response is never bandlimited.
-

Choose *Raised-Cosine* from the menu *Pulse Shape*:

Pulse Shape > Raised-Cosine

Look at raised-cosine pulses with different rolloff factors $0 \leq \alpha \leq 1$. The rolloff factor can be varied using a scrollbar (see Figure 13.17). The green pulse (broken line) included in the plot is the impulse response of the next bit that is transmitted at time T .

TUTORIAL PROBLEM

Problem 13.4 [Raised-Cosine Pulse]

1. For which rolloff factors is the zero ISI condition met? How can this be observed in the impulse response?
2. Which roll-off factors yield a maximum horizontal eye opening? How can this be observed in the impulse response?
3. How does the rolloff factor affect the bandwidth? What is the effect in the time domain?

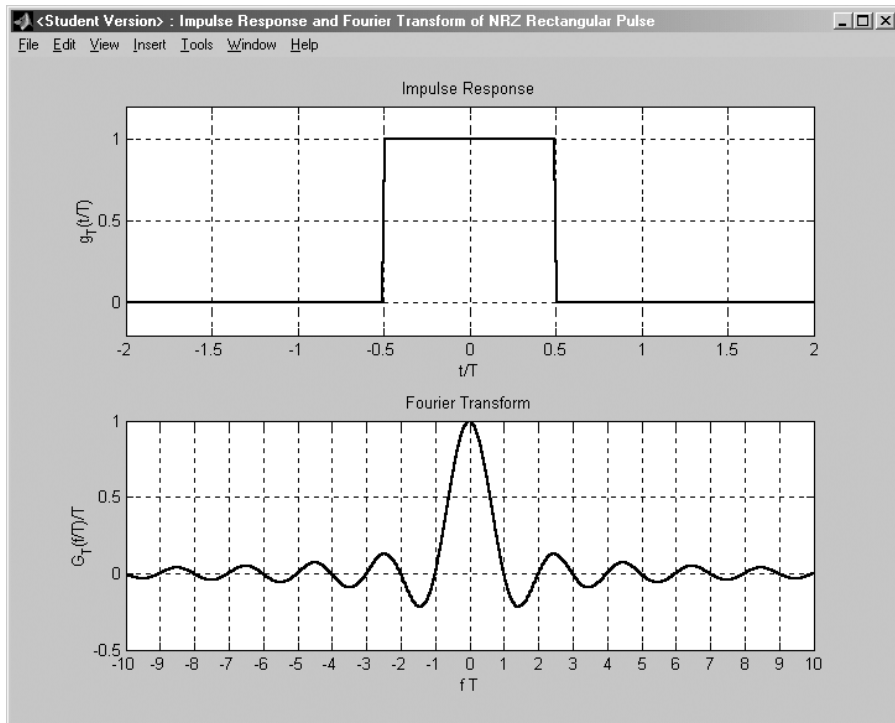


Figure 13.16: Impulse response and Fourier transform of an NRZ rectangular pulse.

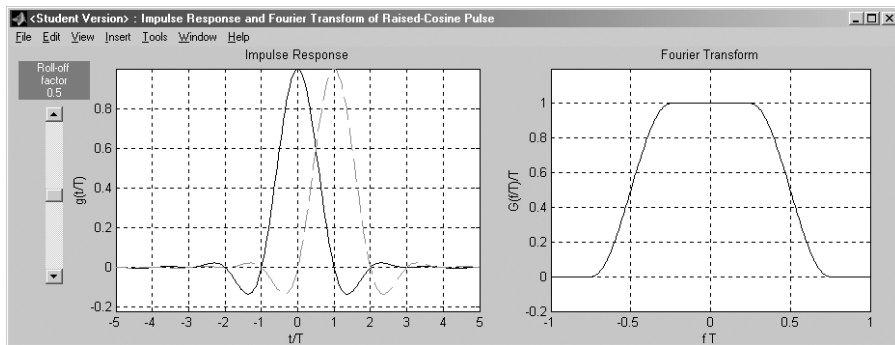


Figure 13.17: Impulse response and Fourier transform of a raised-cosine pulse ($\alpha = 0.5$)

SOLUTION

1. The zero ISI condition is met for all α since the impulse response is zero at nT , $n = 1, 2, 3, \dots$

2. The maximum horizontal eye opening of T is obtained only for $\alpha = 1$. The horizontal eye opening is determined by the transitions $+1 \rightarrow -1$ and $-1 \rightarrow +1$. Since for $\alpha = 1$ the impulse response satisfies

$$g\left(\frac{nT}{2}\right) = \begin{cases} 1, & n = 0 \\ \frac{1}{2}, & n = \pm 1 \\ 0, & \text{otherwise} \end{cases}$$

the respective lines in the eye pattern are zero at $T/2$.

3. The bandwidth increases with increasing α . In the time domain the impulse response is infinite in duration. However, it decreases faster as α decreases.

Now we examine square-root raised-cosine pulses with various roll-off factors (see Figure 13.18). Choose

Pulse Shape > Root-RC

from the *Pulse Shape* menu.

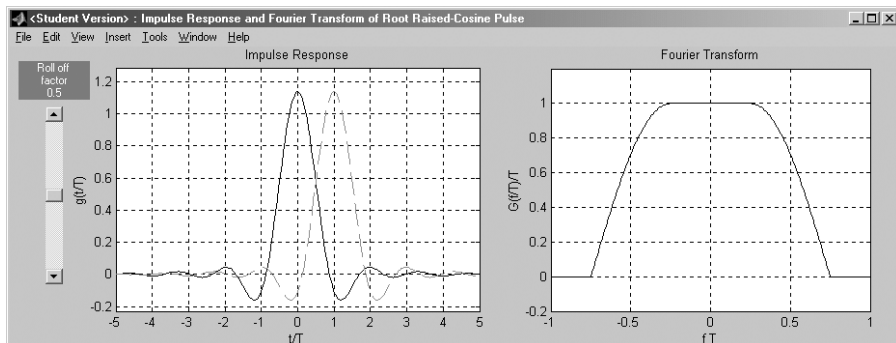


Figure 13.18: Impulse response and Fourier transform of a square-root raised-cosine pulse ($\alpha = 0.5$)

TUTORIAL PROBLEM

Problem 13.5 [Square-Root RC Pulse]

1. Are the zero ISI condition and the maximum horizontal eye-opening condition met?
2. For which rolloff factor are square-root raised-cosine pulses and raised-cosine pulses identical?

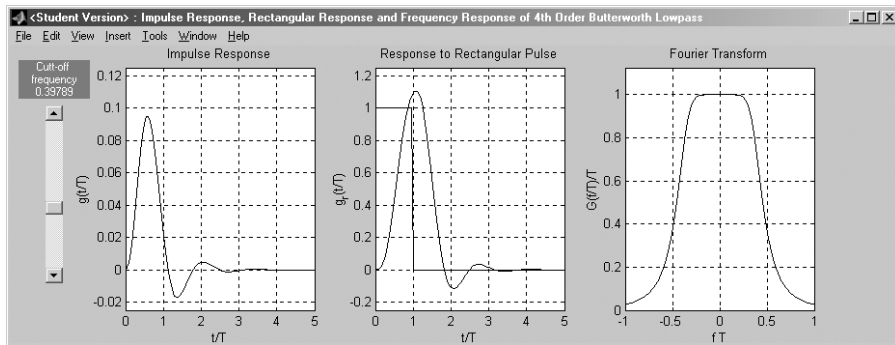


Figure 13.19: Impulse response and Fourier transform of a fourth order Butterworth lowpass

SOLUTION

1. The zero ISI condition is met only for $\alpha = 0$. The horizontal eye opening is always smaller than T .
2. $\alpha = 0$

In the tutorial we sometimes use a fourth order Butterworth receive filter. The impulse response and frequency response of a Butterworth filter are displayed (see Figure 13.19) by

Pulse Shape > Butterworth

The overall impulse response of the transmission scheme is obtained by the convolution

$$g_T(t) * g_R(t) \quad (13.4.7)$$

of the impulse responses of the transmit and receive filter. The overall impulse responses can be viewed from the menu *Convolution* (see Figure 13.20):

Pulse Shape > Convolution > NRZ Rectangular * NRZ Rectangular
 Pulse Shape > Convolution > Raised-Cosine * Raised-Cosine
 Pulse Shape > Convolution > Root-RC * Root-RC

TUTORIAL PROBLEM

Problem 13.6 [Convolution]

1. For which pulse shapes is the zero ISI condition met if a matched filter is used?

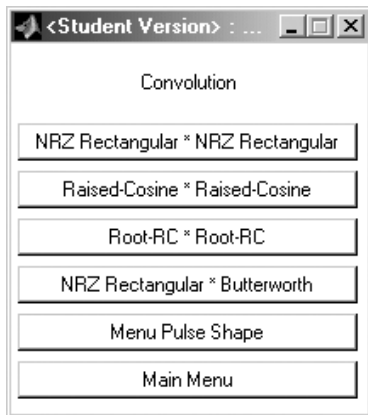
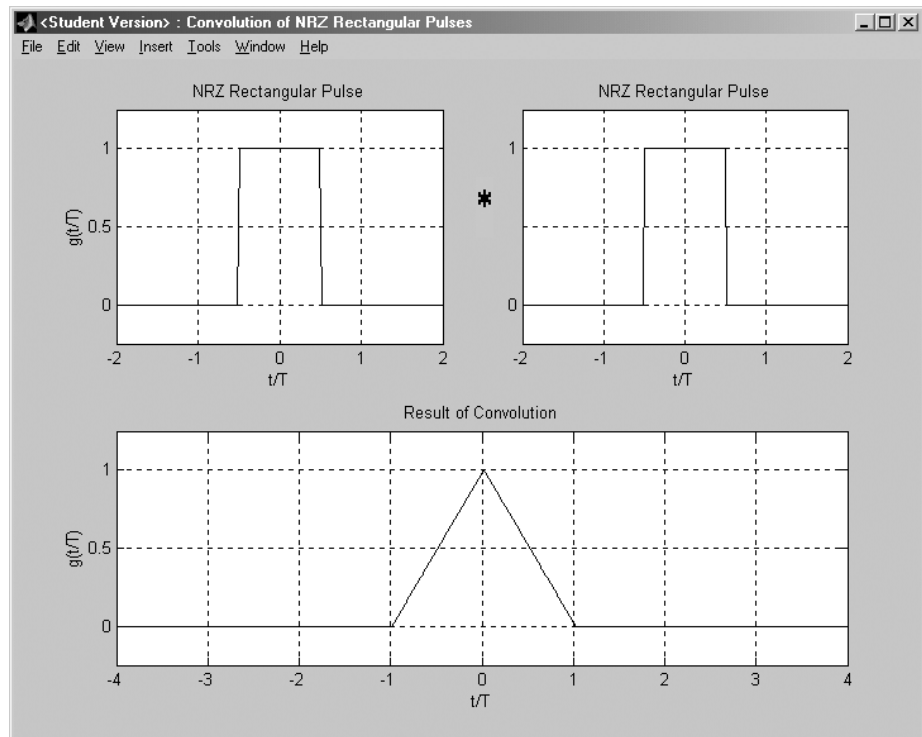
Figure 13.20: Menu *Convolution*

Figure 13.21: Convolution of two NRZ rectangular pulses

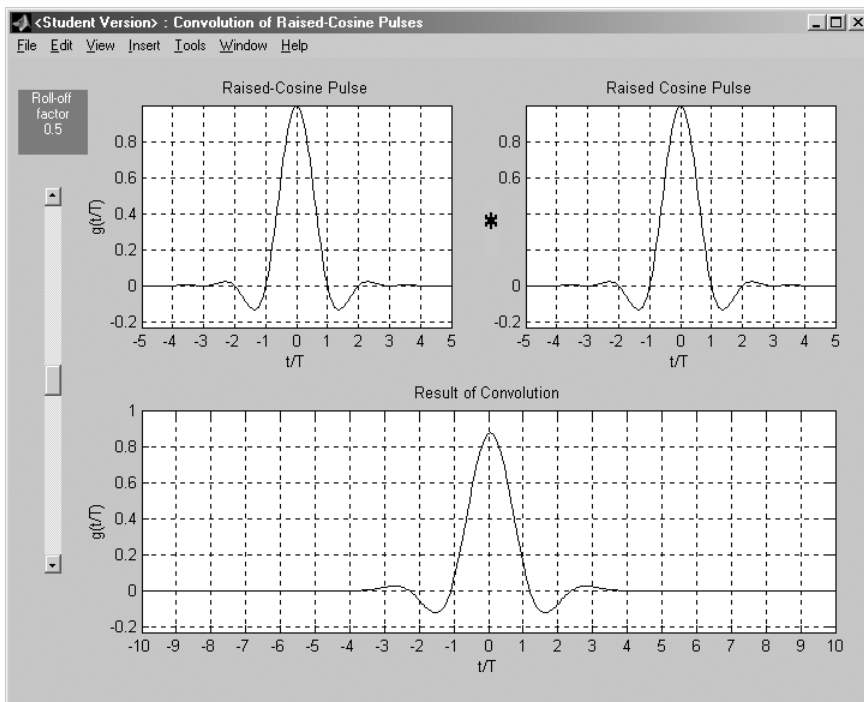


Figure 13.22: Convolution of two raised-cosine pulses ($\alpha = 0.5$)

2. It can be observed that the zero ISI condition is not exactly met for square-root raised-cosine pulses with matched filter and small rolloff factor α . Try to explain!

SOLUTION

1. NRZ Rectangular \ast NRZ Rectangular
 Root-RC \ast Root-RC for all α
 Raised-Cosine \ast Raised-Cosine for $\alpha = 0$.
 2. Square-root raised-cosine pulses have to be implemented with a finite-duration impulse response. For small α the impulse response decreases slowly in the time domain and, therefore, the error due to truncation of the pulse in the time domain becomes noticeable.
-

13.5 Binary Phase-Shift Keying (BPSK)

Binary phase-shift keying (BPSK) serves as a way to get familiar with the Simulink software. Most aspects will be reconsidered in subsequent sections. They are summarized in the guideline on page 606.

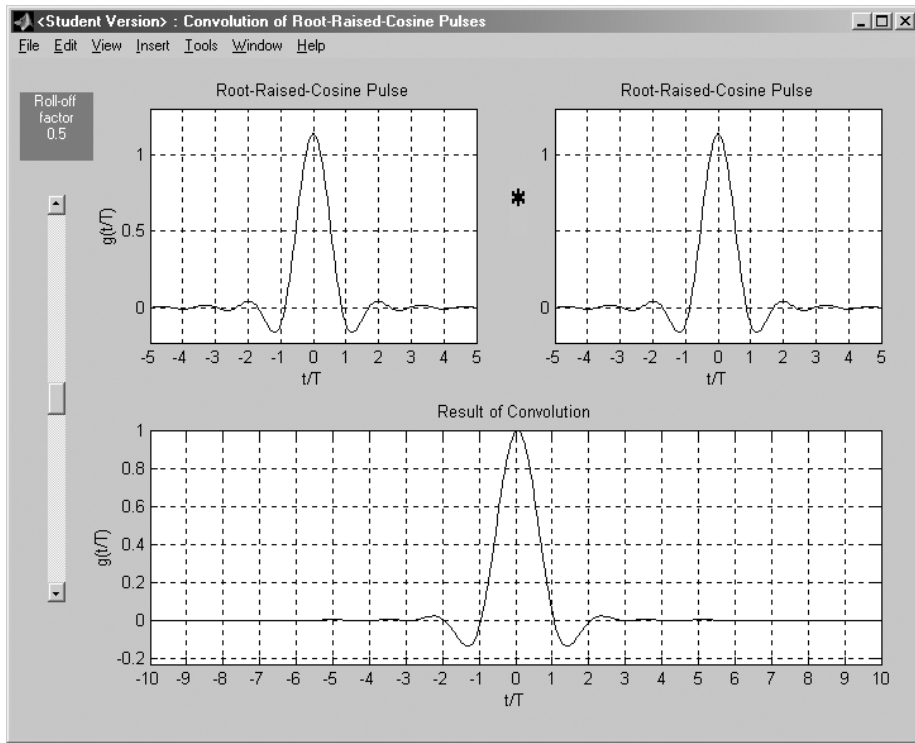


Figure 13.23: Convolution of two square-root raised-cosine pulses ($\alpha = 0.5$)

Choose *BPSK* from the main menu. Another menu will be displayed where you can choose the pulse shape (see Figure 13.24). In the case of NRZ rectangular pulses you can also choose between the matched filter and a Butterworth receive filter (see Figure 13.25). The matched filter is implemented as an integrate and dump filter. If you choose raised-cosine or square-root raised-cosine pulses, the matched filter is used as the receive filter.

13.5.1 Binary Phase Shift Keying with NRZ Rectangular Pulses

Choose NRZ rectangular pulses with matched filter:

BPSK > NRZ Rectangular > Matched Filter

The Simulink model is displayed (see Figure 13.26). A double-click on the blue box *signal-space Constellation* displays the BPSK constellation. Start the simulation from the pulldown menu *Simulation*:

Simulation > Start

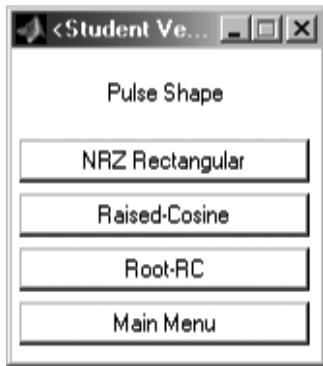


Figure 13.24: *Transmit filter* menu



Figure 13.25: *Receive filter* menu

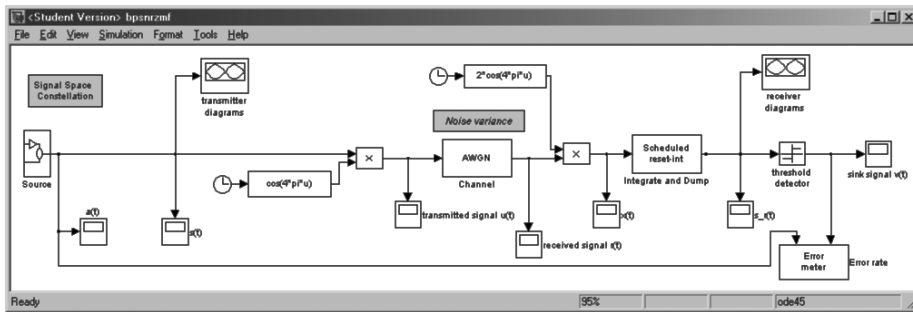


Figure 13.26: Simulink model for BPSK with NRZ rectangular pulses and matched filter

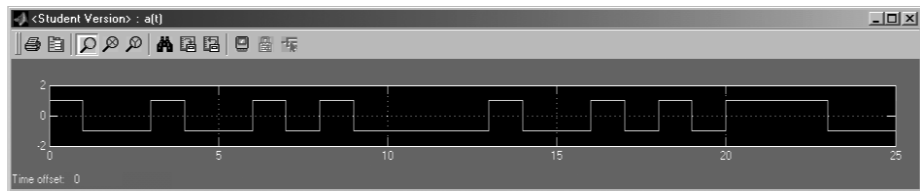
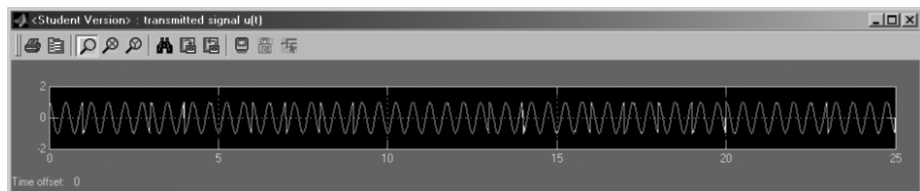
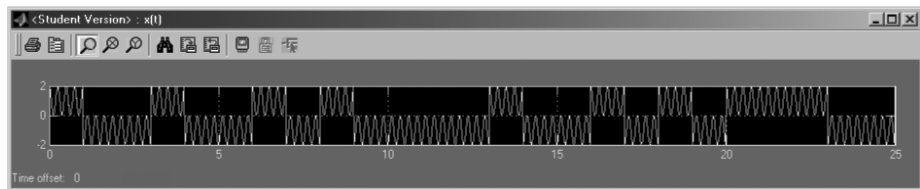
The eye patterns and signal-space diagrams at the transmitter and the receiver are displayed. The respective windows may overlap. You can drag them with the mouse in order to bring another window to the front.

First, look at the time domain signals, which are displayed by a double-click on the respective scopes (see Figures 13.27 to 13.29).

TUTORIAL PROBLEM

Problem 13.7 [BPSK with NRZ Rectangular Pulses and Matched Filter: Time Domain Signals]

1. Is the envelope of the transmitted signal $u(t)$ constant?
2. Explain why the transmitted signal $u(t)$ and the received signal $r(t)$ are not identical.
3. Explain the form of the signal $x(t)$.

Figure 13.27: Source signal $a(t)$.Figure 13.28: Transmitted signal $u(t)$.Figure 13.29: Signal $x(t)$ at matched filter input

SOLUTION

1. The envelope is constant.
2. The received signal is corrupted by additive noise (AWGN channel).
3. After demodulation the signal $x(t)$ contains also a component at $2f_c$:

$$\begin{aligned} x(t) &= s(t) \cos(2\pi f_c t) \cdot 2 \cos(2\pi f_c t) \\ &= s(t)(1 + \cos(4\pi f_c t)) \text{ plus noise} \end{aligned}$$

Now, look at the eye patterns and signal-space plots (see Figures 13.30 to 13.34).

The green trajectory describes the baseband signal after pulse shaping in the signal-space (see Figure 13.30). The blue signal-space points in the scatter plot (see Figure 13.31) are obtained by sampling the green trajectory at the symbol rate at the optimum sampling time, i.e., at maximum vertical eye opening. In the case of zero ISI we obtain exactly the signal-space constellation points. The trajectory describes the transitions between the constellation points.

First, look at the transmitter plots.

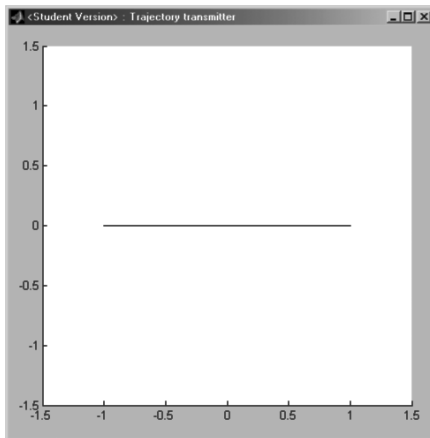


Figure 13.30: Transmitter trajectory for BPSK with NRZ rectangular pulses

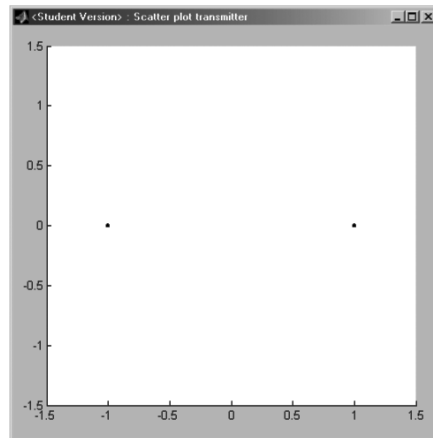


Figure 13.31: Transmitter scatter plot (signal-space constellation) for BPSK with NRZ rectangular pulses

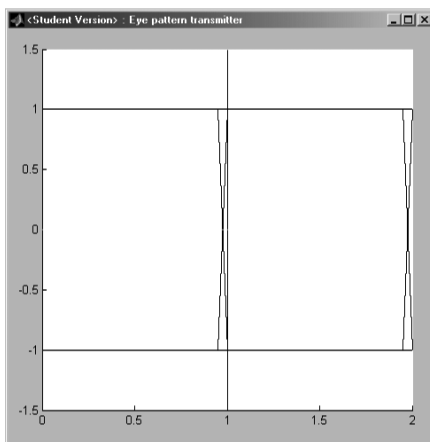


Figure 13.32: Eye pattern at transmitter for BPSK with NRZ rectangular pulses

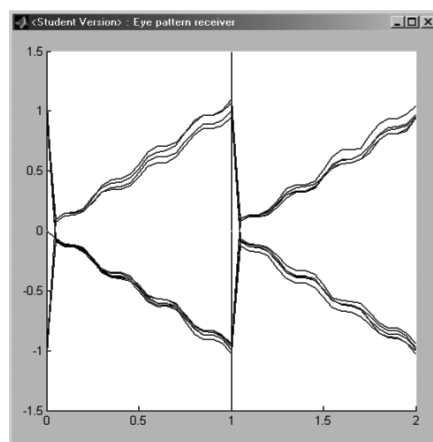


Figure 13.33: Eye pattern at receiver for BPSK with NRZ rectangular pulses and matched filter

TUTORIAL PROBLEM

Problem 13.8 [BPSK with NRZ Rectangular Pulses and Matched Filter: Transmitter Trajectory, Scatter Plot, and Eye Pattern]

1. Is the zero ISI condition met at the transmitter? How can this be observed in the eye pattern and the scatter plot?
2. Is the horizontal eye opening maximum?

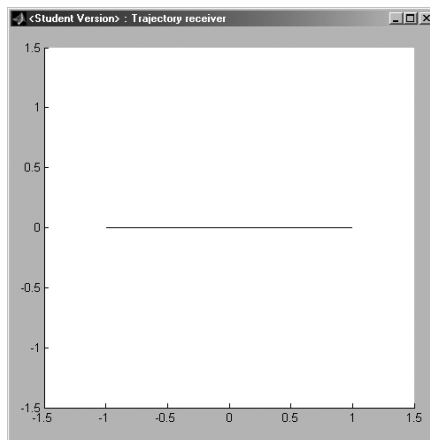


Figure 13.34: Receiver trajectory for BPSK with NRZ rectangular pulses and matched filter

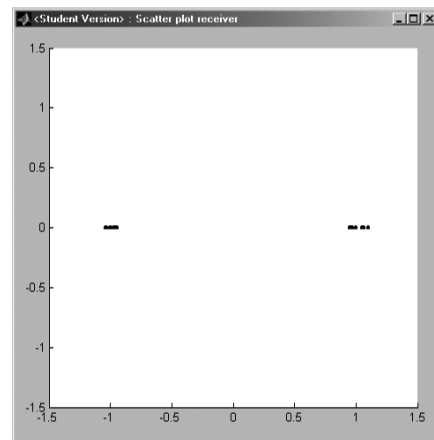


Figure 13.35: Receiver scatter plot for BPSK with NRZ rectangular pulses and matched filter

SOLUTION

1. Yes. The maximum vertical eye opening is obtained. Sampling of the trajectory at the optimum sampling time yields the BPSK constellation points.
2. Yes.

Now, we examine the respective diagrams at the receiver.

TUTORIAL PROBLEM

Problem 13.9 [BPSK with NRZ Rectangular Pulses and Matched Filter: Receiver Trajectory, Scatter Plot, and Eye Pattern]

1. Explain the form of the eye pattern.
2. Are vertical and horizontal eye openings maximum?
3. What is the optimum sampling time?
4. Why do we observe more than two signal-space points in the scatter plot at the receiver?

SOLUTION

1. The receive filter is implemented as an integrate and dump filter. The waves result from the integration of $x(t)$. Furthermore, the noise is contained in the received signal.
2. Due to additive noise we do not observe the maximum horizontal and vertical eye opening.

3. $t/T = 0, 1, 2, \dots$
4. Because of additive noise.

We now consider noiseless transmission. To change the variance of the AWGN, double-click on the blue box *Noise variance* in the Simulink model. A scrollbar is displayed where you can adapt the noise to the smallest possible value (zero is not possible since singularities would result). Restart the simulation from the pulldown menu:

Simulation > Stop
Simulation > Start

TUTORIAL PROBLEM

Problem 13.10 [Noiseless BPSK Transmission with NRZ Rectangular Pulses and Matched Filter]

1. How do the transmitted signal $u(t)$ and the received signal $r(t)$ differ now?
2. Which modifications do you observe in the eye patterns and scatter plots?

SOLUTION

1. $u(t)$ and $r(t)$ are now identical.
2. No modifications at the transmitter plots. Since no noise is present at the receiver, the eye opening is maximum and sampling of the trajectory yields the BPSK signal constellation points. (Slight inaccuracy is due to the integration.)

Go back to the main menu and choose a Butterworth lowpass as a receive filter instead of the matched filter:

BPSK > NRZ Rectangular > Butterworth

Compare the source signal $a(t)$ and the sink signal $v(t)$. To do so, place the source signal window directly above the sink signal window.

TUTORIAL PROBLEM

Problem 13.11 [BPSK with NRZ Rectangular Pulses and Butterworth Receive Filter]

1. Explain the delay between $a(t)$ and $v(t)$.
2. Do you observe detection errors?
3. Repeat Problems 13.9 and 13.10 for the Butterworth receive filter.

SOLUTION

1. The Butterworth lowpass is a partial response filter that in a causal implementation introduces delay.
2. Depends on the noise variance.
3.
 - The shape of the eye pattern is determined by filtering with the Butterworth filter. Furthermore, noise is present.
 - The zero ISI condition is not met due to the Butterworth filter.
 - Optimum sampling time at maximum vertical eye opening.
 - Since the zero ISI condition is not met, the received signal-space points scatter even if no noise is present.

Now you know how to use the software. In the following sections we will describe only new aspects and point out what should be noticed.

13.5.2 Binary Phase Shift Keying with Raised-Cosine Pulses

In this section we investigate BPSK with raised-cosine pulses. Choose

BPSK > Raised-Cosine

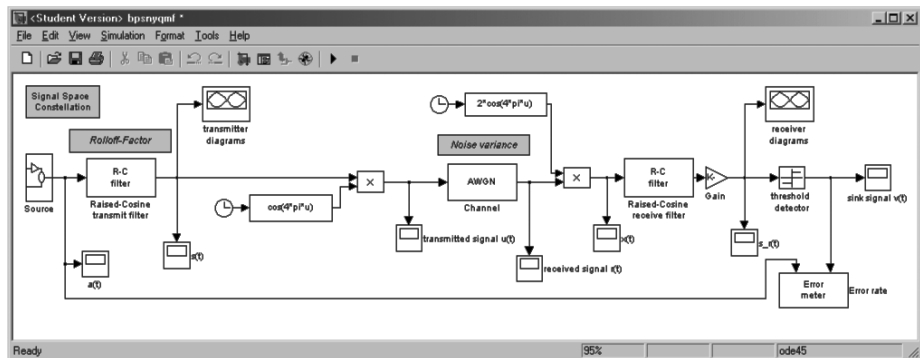
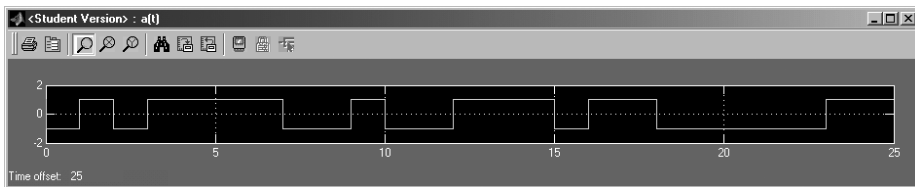
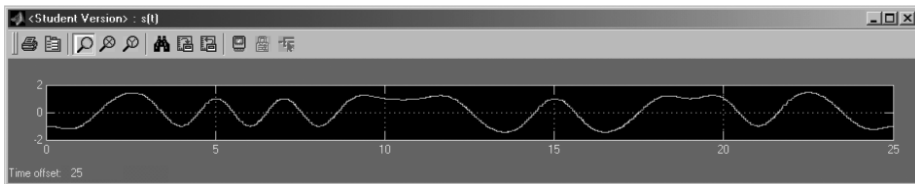
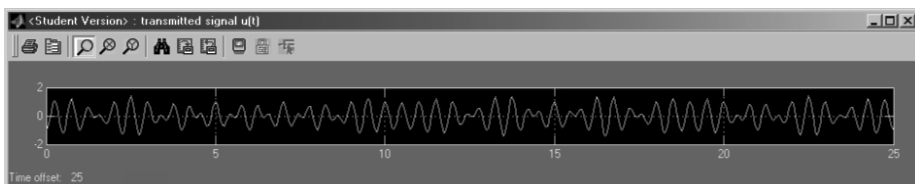


Figure 13.36: Simulink model for BPSK with raised-cosine pulses and matched filter

Figure 13.36 shows the Simulink model. The rolloff factor is set to $\alpha = 0.5$ and the filter delay is six symbol durations, $6T$. You should keep these settings throughout the tutorial. However, you can change the settings using a scrollbar which is opened by a double-click on the blue block *Rolloff-Factor*.

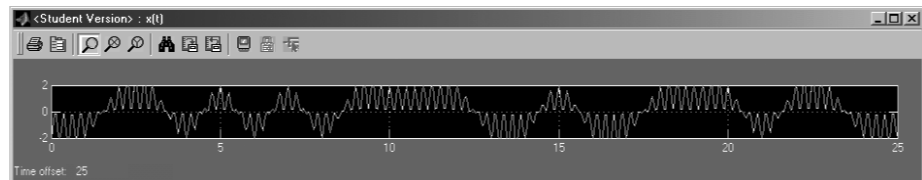
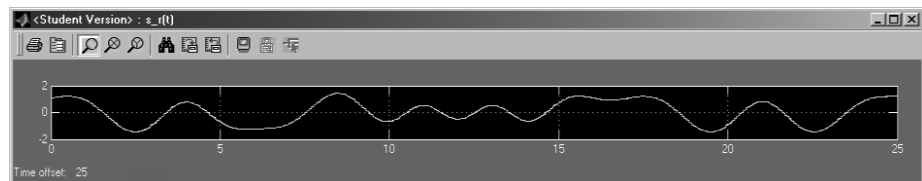
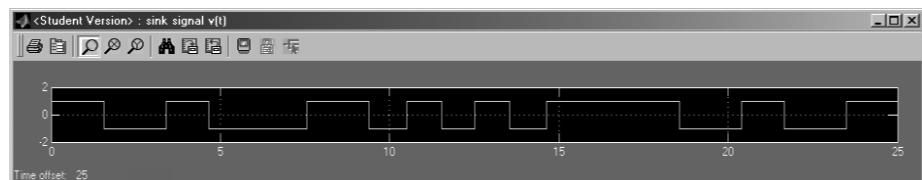
Set the noise variance to a very small value. The time domain signals, eye patterns, and scatter plots are depicted in Figures 13.37 to 13.46.

Figure 13.37: Source signal $a(t)$ Figure 13.38: Baseband signal $s(t)$ Figure 13.39: Transmitted signal $u(t)$

TUTORIAL PROBLEM

Problem 13.12 [BPSK with Raised-Cosine Pulses]

1. Are the zero ISI condition and the maximum horizontal eye-opening condition met at the transmitter and receiver?
2. What does the answer to question 1 mean for the detection? Consider the eye pattern at the receiver. Does it make sense to use a raised-cosine filter at the transmitter and a matched filter at the receiver?
3. Why is the signal-space trajectory not limited to the range between +1 and -1?
4. How does the transmitted signal $u(t)$ change compared to NRZ rectangular pulses? What is the effect of bandlimitation on the transmitted signal?
5. Compare the source signal $a(t)$ and the sink signal $v(t)$. Are there errors? (Take the filter delays into consideration!)

Figure 13.40: Signal $x(t)$ at matched filter inputFigure 13.41: Demodulated baseband signal $s_r(t)$ at matched filter outputFigure 13.42: Sink signal $v(t)$

SOLUTION

1. The zero ISI condition is met only at the transmitter because the cascade of two raised-cosine pulses (matched filter!) results in ISI if $\alpha \neq 0$. Also, the horizontal eye opening is not maximum. We would observe maximum horizontal eye opening at the transmitter for $\alpha = 1$ (see Tutorial Problem 13.4).
2. The detectability would be optimum after the transmit filter. However, after the receive filter we encounter ISI, resulting in a reduced vertical eye opening. Therefore, the raised-cosine pulses and a matched receive filter are not optimum. The raised-cosine pulse shaping has to be split evenly between the transmit and receive filters in order to simultaneously meet the matched filter condition, which maximizes the SNR at the receive filter output and the zero ISI condition. Therefore, we need to apply a square-root raised-cosine pulse. Then, the zero ISI condition is met at the receiver rather than at the transmitter.
3. This is due to the raised-cosine pulse shape. The range of the signal-space trajectory is the same as in the vertical axis of the eye pattern.

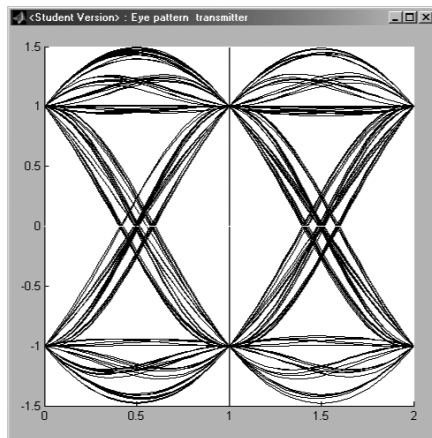


Figure 13.43: Eye pattern at the transmitter for BPSK with raised-cosine pulses

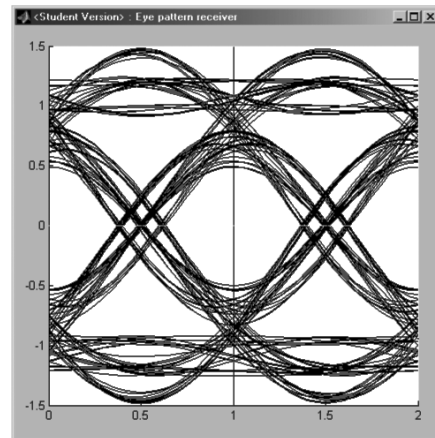


Figure 13.44: Eye pattern at the receiver for BPSK with raised-cosine pulses

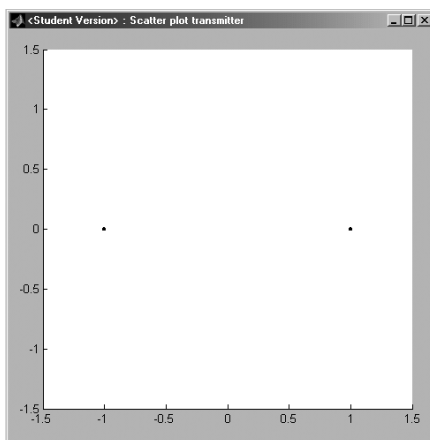


Figure 13.45: Transmitter scatter plot for BPSK with raised-cosine pulses

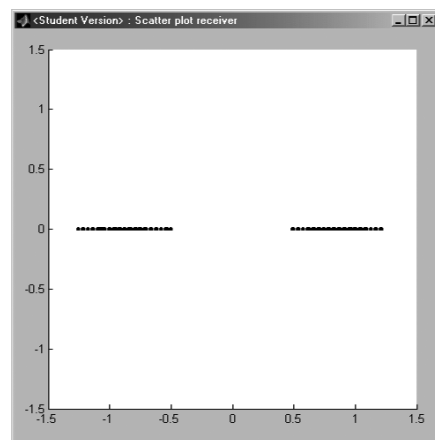


Figure 13.46: Receiver scatter plot for BPSK with raised-cosine pulses

4. The envelope of $u(t)$ is not constant anymore. Bandlimitation results in an additional amplitude modulation. Rectangular phase shift keying requires infinite bandwidth. Modulated signals with constant envelope always require infinite bandwidth. This applies, for example, to frequency-modulated signals.
5. The sink signal is delayed by the transmit and receive filter delays of $2 \cdot 6T = 12T$. The number of errors depends on the noise variance.

13.5.3 Binary Phase Shift Keying with Square-Root Raised-Cosine Pulses

Choose

BPSK > Root-RC

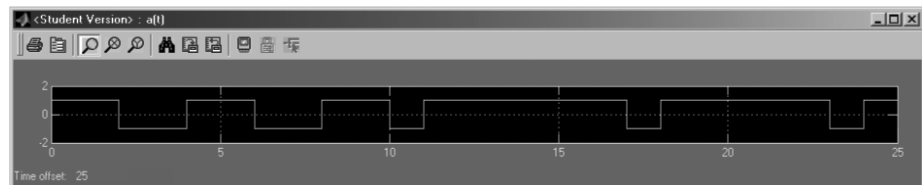


Figure 13.47: Source signal $a(t)$

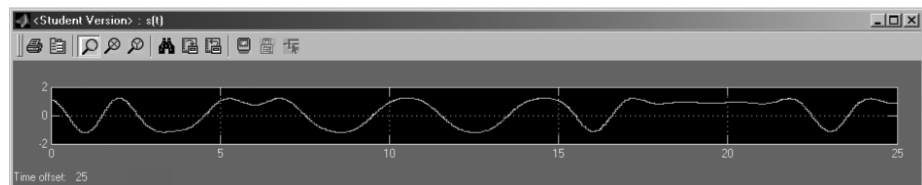


Figure 13.48: Baseband signal $s(t)$

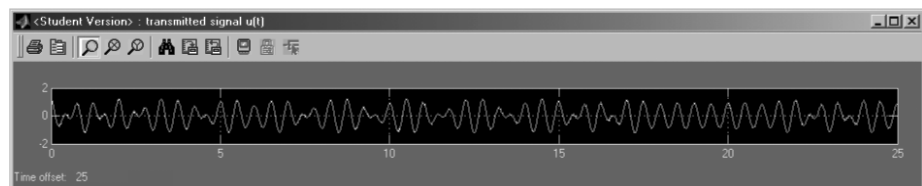


Figure 13.49: Transmitted signal $u(t)$

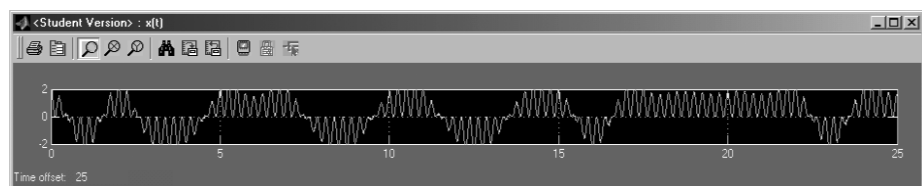


Figure 13.50: Signal $x(t)$ at matched filter input

in order to investigate BPSK with square-root raised-cosine pulses. The time domain signals, eye patterns, and scatter plots are depicted in Figures 13.47 to 13.56.

Carry out the same experiments as in the previous section for raised-cosine pulses. Note that now the zero ISI condition is met at the matched filter output. Therefore, in the sequel we will only consider the relevant case of a square-root raised-cosine transmit filter.

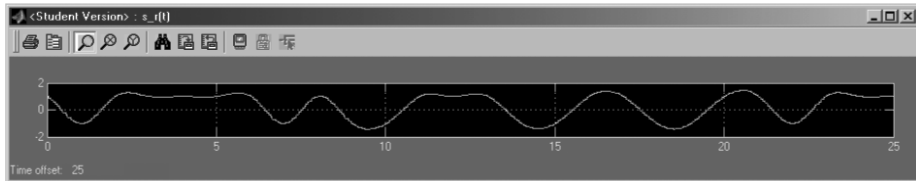


Figure 13.51: Demodulated baseband signal $s_r(t)$ at matched filter output

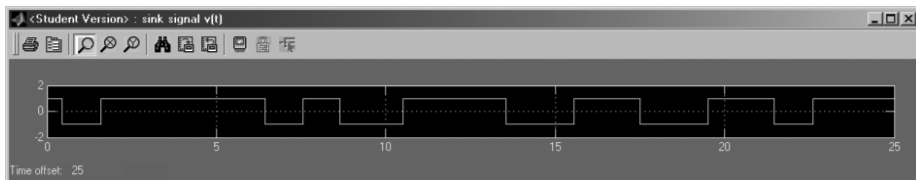


Figure 13.52: Sink signal $v(t)$

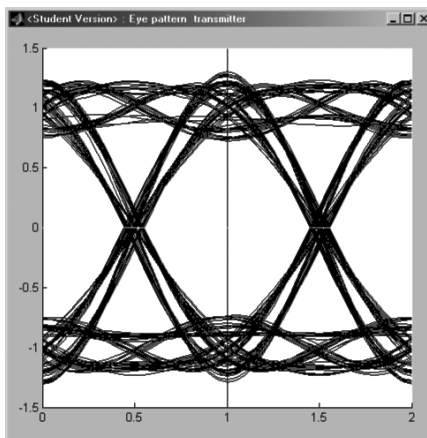


Figure 13.53: Eye pattern at the transmitter for BPSK with square-root raised-cosine pulses

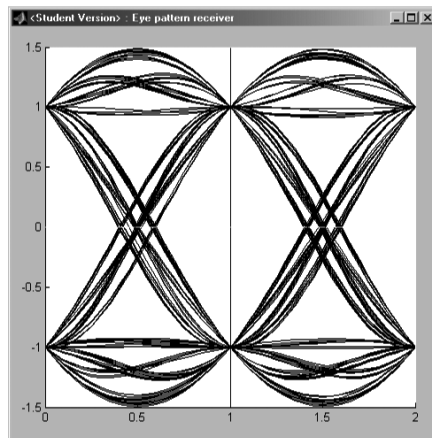


Figure 13.54: Eye pattern at the receiver for BPSK with square-root raised-cosine pulses

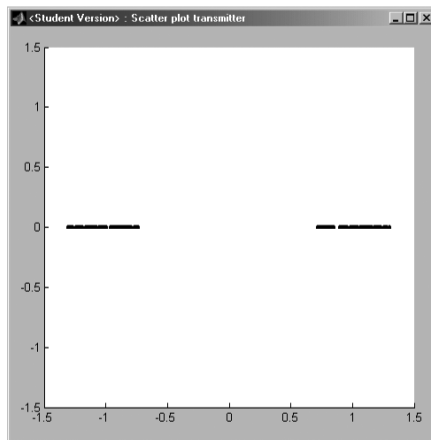


Figure 13.55: Transmitter scatter plot for BPSK with square-root raised-cosine pulses

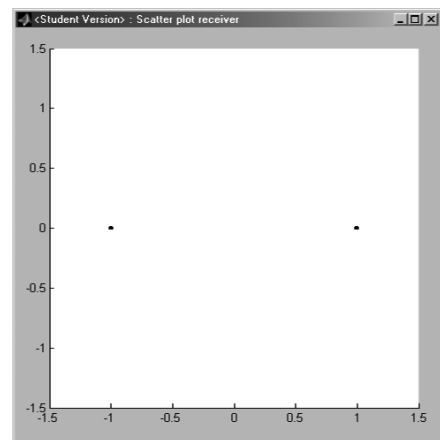


Figure 13.56: Receiver scatter plot for BPSK with square-root raised-cosine pulses

Guideline

Several aspects that have been examined for BPSK can also be considered for other modulation schemes. Therefore, we summarize the most important points in the following list, which serves as a guideline for the tutorial. In the following sections we will mention only new or important aspects.

1. First, select a very small noise variance. Later consider also the effect of noise.
2. Is the zero ISI condition met at the transmitter (use eye pattern and signal-space plots)?
3. Is the horizontal eye opening maximum at the transmitter (use eye pattern)?
4. Is the zero ISI condition met at the receiver ?
5. Is the horizontal eye opening maximum at the receiver ?
6. Is the envelope of the transmitted signal constant ? (explain influence of pulse shaping and bandlimitation !)?
7. Inspect the demodulated signal before and after the lowpass receive filter.
8. Observe the signal-space trajectory and explain its behavior (zero ISI condition). Which transitions are possible ? What range in the signal-space is covered ?
9. Inspect the eye patterns (Determine the optimal sampling time, shape of the eye pattern, vertical eye opening, effect of additive noise.).
10. Do bit errors occur? (Examine with different noise variance, effect of vertical eye opening and zero ISI condition.)

13.6 Quadrature Phase-Shift Keying (QPSK)

13.6.1 Quadrature Phase-Shift Keying with Square-Root Raised-Cosine Pulses

Examine QPSK with square-root raised-cosine pulses:

QPSK > Root-RC

The Simulink model is depicted in Figure 13.57. The transmitter and receiver models depicted in Figure 13.58 and Figure 13.59 are opened by a double-click on the blue box *Transmitter* or *Receiver*, respectively.

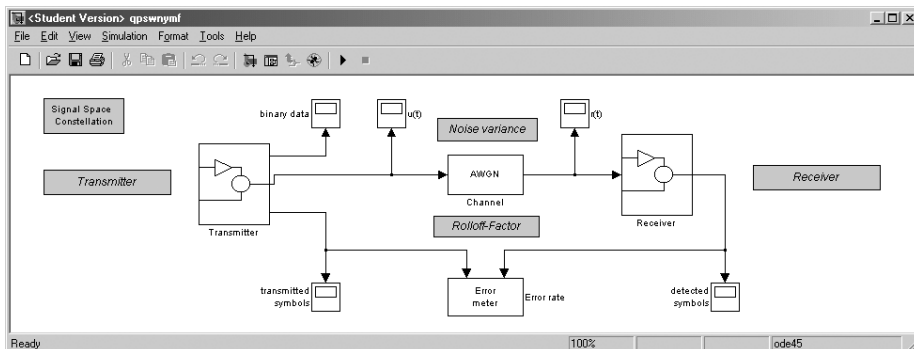


Figure 13.57: Simulink model for QPSK with square-root RC pulses

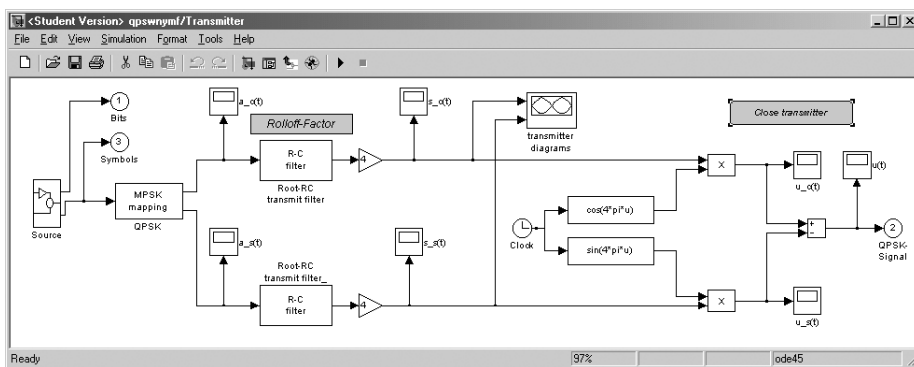


Figure 13.58: Simulink model for QPSK transmitter with square-root RC pulses

Open the transmitter and start the simulation. Note that now separate eye patterns are displayed for both quadrature components that are identical to the respective BPSK eye patterns in Figures 13.53 and 13.54. The time domain signals in both quadrature components look like the respective BPSK signals. The QPSK signals are shown in

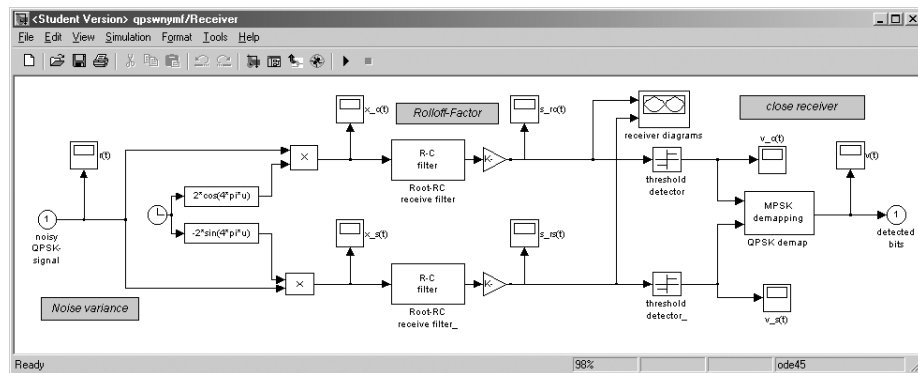
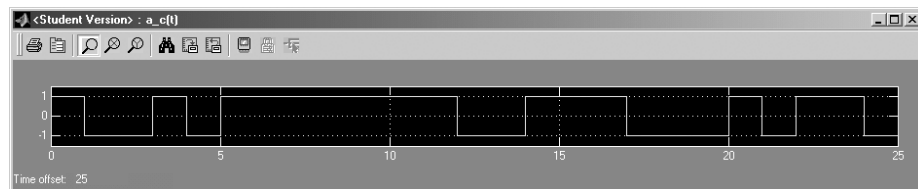
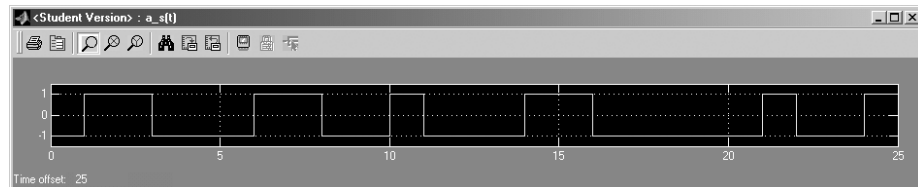


Figure 13.59: Simulink model for QPSK receiver with square-root RC pulses

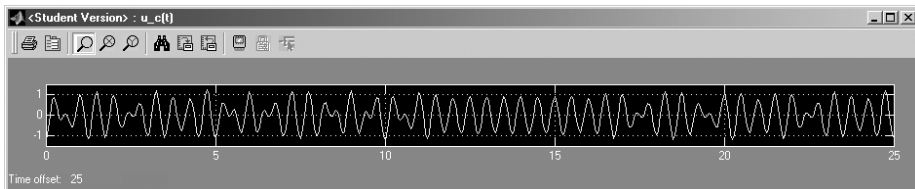
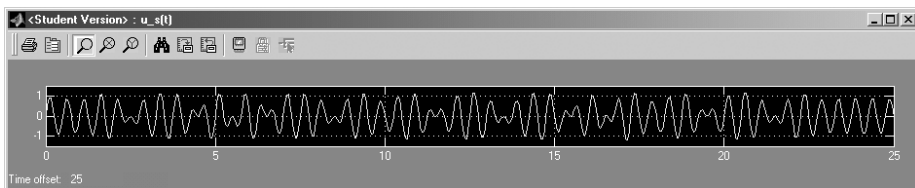
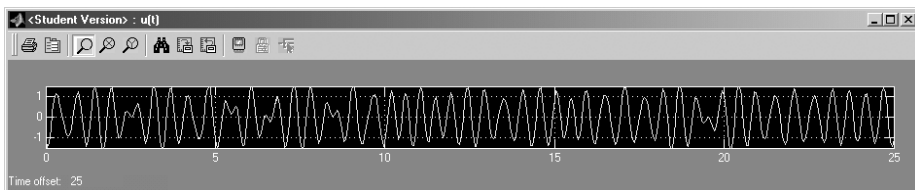
Figure 13.60: In-phase source signal $a_c(t)$ Figure 13.61: Quadrature source signal $a_s(t)$

Figures 13.60 to 13.68 for noiseless transmission. The scatter plot observed at the receiver in noisy channels looks similar to Figure 13.67. Inspect the envelope of the modulated signals in the quadrature components and of the transmitted signal $u(t)$.

TUTORIAL PROBLEM

Problem 13.13 [QPSK with Square-Root Raised-Cosine Pulses: Transmitter]

1. Explain the behavior of the trajectory at the transmitter.
2. Try to find fades in the envelope of the transmitted signal $u(t)$ and give reasons considering the respective signal-space transitions. (Take the transmit filter delay of $6T$ into consideration.)

Figure 13.62: In-phase component $u_c(t)$ of transmitted signalFigure 13.63: Quadrature component $u_s(t)$ of transmitted signalFigure 13.64: Transmitted signal $u(t)$

SOLUTION

1. Since the zero ISI condition is not met at the transmitter, the trajectory shows no nodes in the four QPSK signal-space constellation points.
2. The envelope fades if both quadrature components change simultaneously. In this case the trajectory performs a diagonal transition through or close to the origin. Due to the bandlimitation, the shift keying between constellation points is not rectangular, which results in envelope fades. A simple method to reduce amplitude fades is Offset-QPSK, which is covered in Section 13.7.

Double-click on the blue box *Close transmitter* and then *Receiver* to simulate the receiver.

TUTORIAL PROBLEM

Problem 13.14 [QPSK with Square-Root Raised-Cosine Pulses: Receiver] What do you observe in the eye patterns and in the signal-space plots?

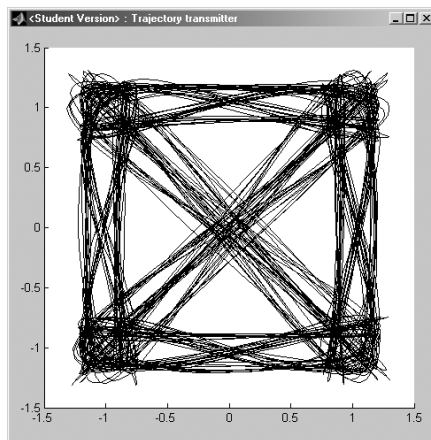


Figure 13.65: Transmitter trajectory for QPSK

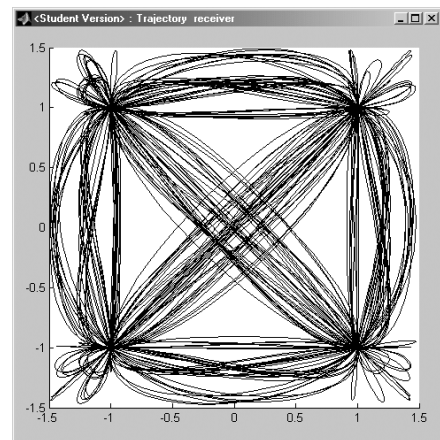


Figure 13.66: Receiver trajectory for QPSK

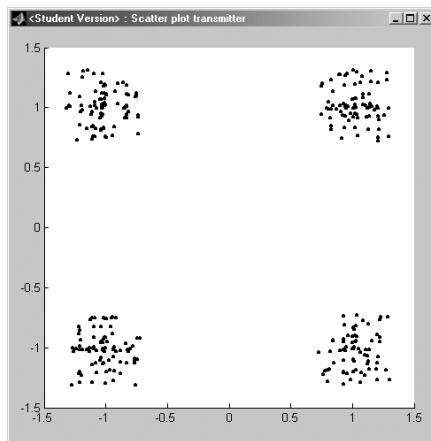


Figure 13.67: Transmitter scatter plot for QPSK

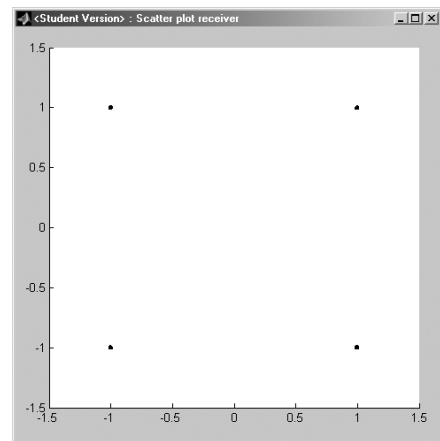


Figure 13.68: Receiver scatter plot for QPSK

SOLUTION

Eye pattern: Maximum eye opening at sampling time. All lines cross in two points at the sampling time.

Trajectory: The lines cross in the QPSK constellation points if no noise is present.

Scatter plot: QPSK constellation points.

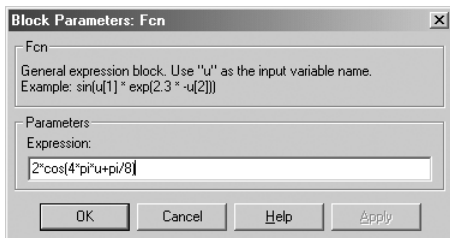


Figure 13.69: Cos carrier parameter window

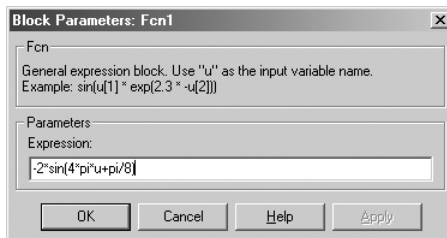


Figure 13.70: Sin carrier parameter window

13.6.2 Phase and Frequency Offset

We now encounter demodulation with phase and frequency mismatch for QPSK with square-root raised-cosine pulses. Reduce the noise variance to the smallest value and open the *Receiver* model.

Phase Offset

Double-click on the Simulink block of the cos carrier at the receiver. The parameter window is displayed. Introduce a phase offset of $\varphi = \pi/8$ in both quadrature components, as shown in Figures 13.69 and 13.70 (u denotes the frequency). Restart the simulation. The signal-space diagrams and eye patterns at the receiver are depicted in Figures 13.71 to 13.74.

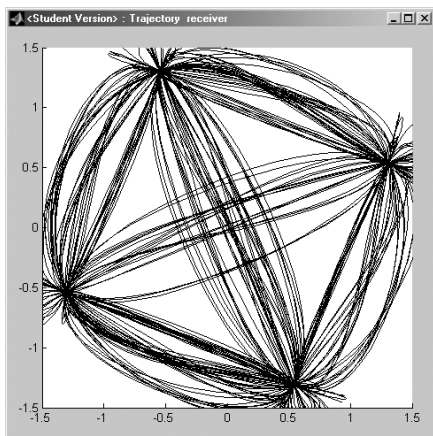


Figure 13.71: Receiver trajectory for QPSK with phase offset

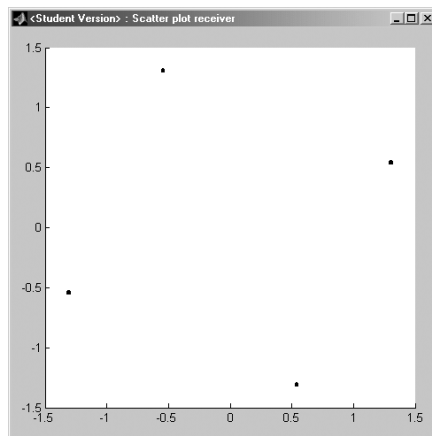


Figure 13.72: Receiver scatter plot for QPSK with phase offset

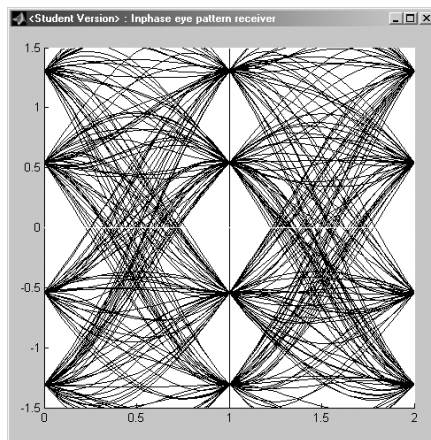


Figure 13.73: Eye pattern in in-phase component for QPSK with phase offset

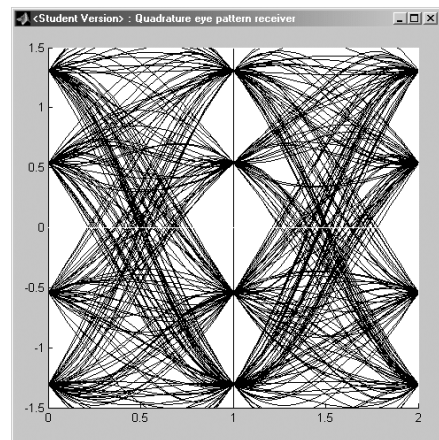


Figure 13.74: Eye pattern in quadrature component for QPSK with phase offset

TUTORIAL PROBLEM

Problem 13.15 [QPSK with Phase Offset]

1. What is the effect on the receiver scatter plot and the trajectory?
2. For which range of φ is error-free detection possible if no noise is present and φ is unknown to the receiver?
3. Explain the effects in the eye patterns.

SOLUTION

1. Scatter plot and trajectory are rotated by φ .
2. $-\pi/4 < \varphi < \pi/4$
3. At the sampling time now four values are possible in both quadrature components. This can also be seen from the received signal-space points in Figure 13.72.

We now examine what happens if the demodulating carriers in both quadrature components (\cos and \sin) are not exactly shifted by 90° . Reset the phase shift in the \sin carrier component only to $\varphi = 0$ (see Figures 13.75 and 13.76).

The resulting diagrams are depicted in Figures 13.77 to 13.80.

TUTORIAL PROBLEM

Problem 13.16 [QPSK with Phase Mismatch] Describe the effect in the scatter plot.

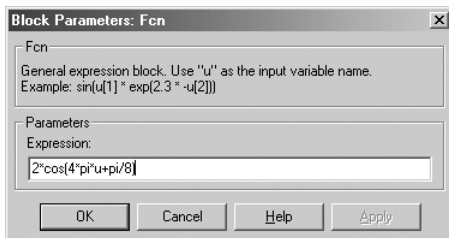


Figure 13.75: Cos carrier parameter window

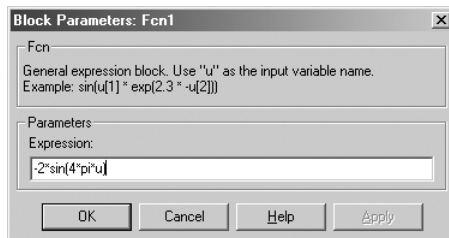


Figure 13.76: Sin carrier parameter window

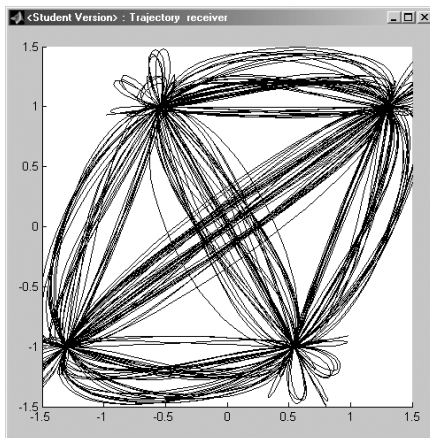


Figure 13.77: Receiver trajectory for QPSK with phase offset in cos component

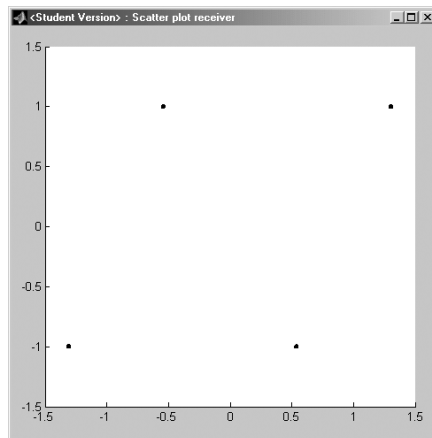


Figure 13.78: Receiver scatter plot for QPSK with phase offset in cos component

SOLUTION

At the sampling time only the correct values ± 1 occur in the sin component. In the cos component we still observe four possible values. Therefore, the received signal-space constellation is distorted.

Frequency Offset

In order to investigate a frequency offset, modify the demodulating carriers according to Figures 13.81 and 13.82. Figures 13.83 to 13.86 show the resulting signal-space diagrams and eye patterns.

TUTORIAL PROBLEM

Problem 13.17 [QPSK with Frequency Offset] Describe the eye patterns and signal-space plots. Is error-free detection possible?

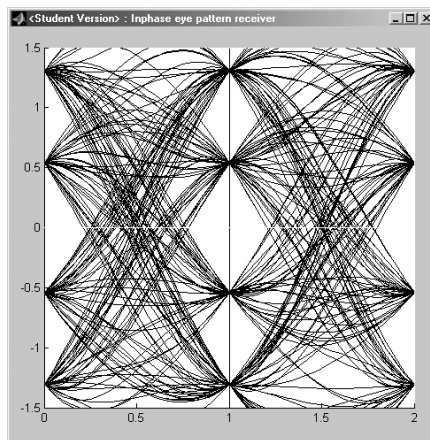


Figure 13.79: Eye pattern in in-phase component for QPSK with phase offset in cos component

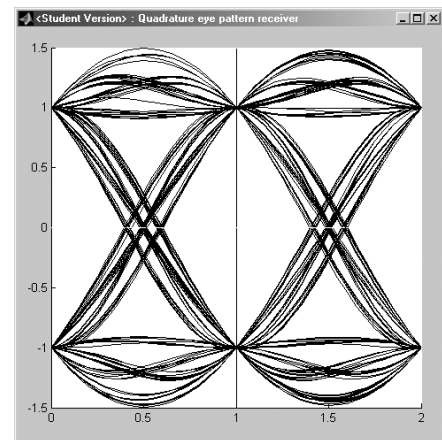


Figure 13.80: Eye pattern in quadrature component for QPSK with phase offset in cos component

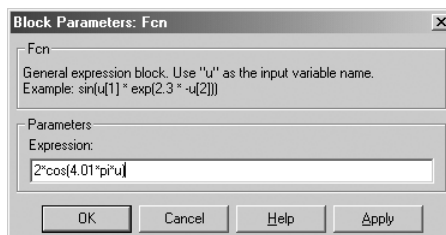


Figure 13.81: Cos carrier parameter window

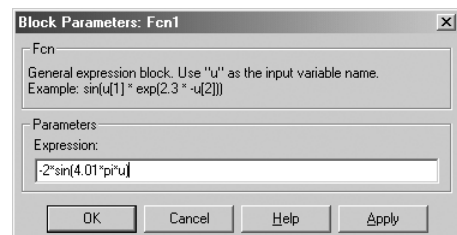


Figure 13.82: Sin carrier parameter window

SOLUTION

The received signal-space constellation rotates according to the frequency offset Δf . Detection is not possible. This can also be concluded from the chaotic behavior of the trajectory and the eye patterns.

13.7 Offset-QPSK

13.7.1 Theory

In Problem 13.13 we encountered the problem of envelope fades in QPSK-modulated signals. If two successive symbols are symmetric in the origin of the signal-space constellation, the trajectory performs a diagonal transition through the origin. This results

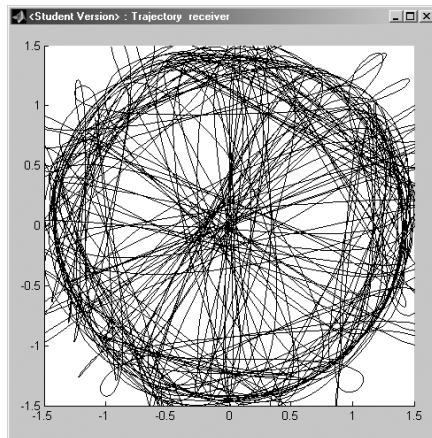


Figure 13.83: Receiver trajectory for QPSK with frequency offset

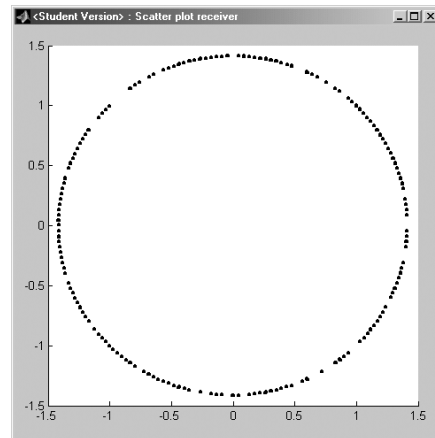


Figure 13.84: Receiver scatter plot for QPSK with frequency offset

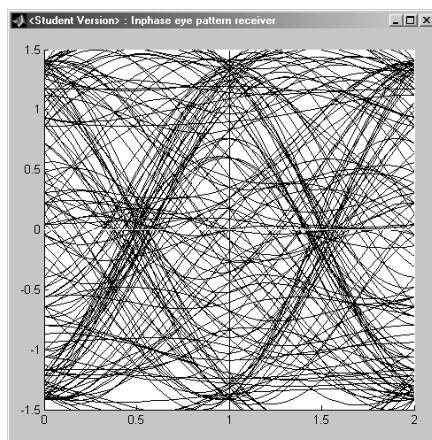


Figure 13.85: Eye pattern in in-phase component for QPSK with frequency offset

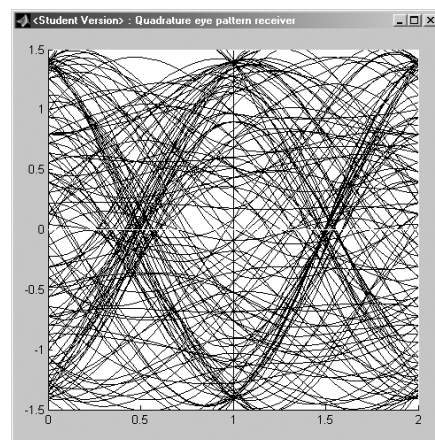


Figure 13.86: Eye pattern in quadrature component for QPSK with frequency offset

in amplitude fading of the transmitted signal. Consequently, the transmitted signal becomes sensitive to nonlinear distortions during transition as imposed by amplifiers. Therefore, many applications require a close to constant envelope of the transmitted signal. A simple method to avoid deep fades is Offset-QPSK.

In Offset-QPSK, the quadrature component of a QPSK signal is delayed by $T/2$ with respect to the in-phase component. Hence, the in-phase and the quadrature components cannot change simultaneously anymore, and diagonal transitions of the trajectory are avoided.

13.7.2 Experiments

Examine Offset-QPSK with square-root raised-cosine pulses:

Offset-QPSK > Root-RC

The basic Simulink model is the same as depicted in Figure 13.57 for QPSK. The only modification at the transmitter is the delay of $T/2$ in the quadrature component (see Figure 13.87). At the receiver the in-phase component is delayed by $T/2$ to restore the QPSK constellation (see Figure 13.88). The Offset-QPSK signals and diagrams are depicted in Figures 13.89 to 13.99.

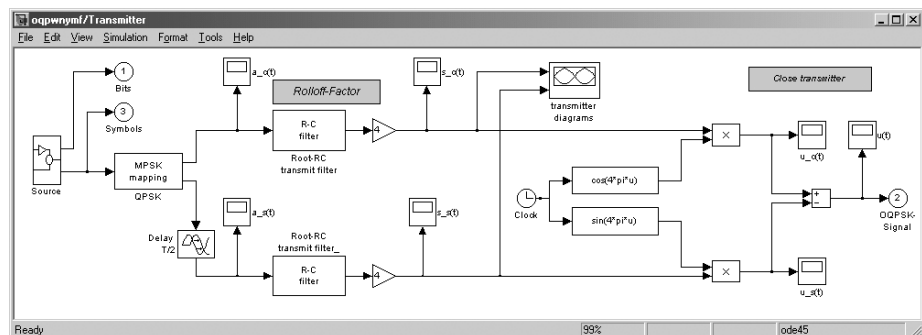


Figure 13.87: Simulink model for Offset-QPSK transmitter with square-root RC pulses

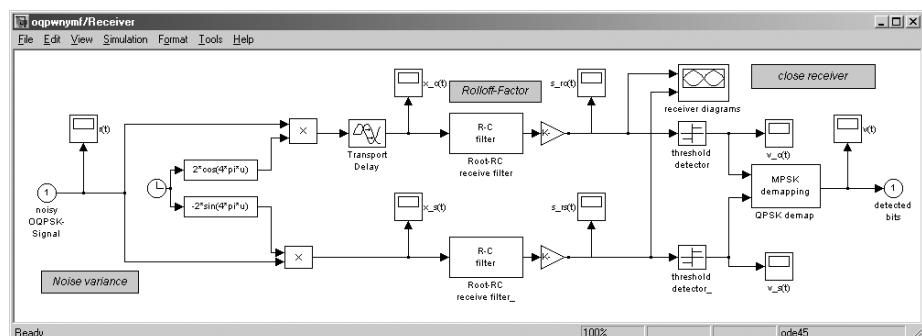


Figure 13.88: Simulink model for Offset-QPSK receiver with square-root RC pulses

TUTORIAL PROBLEM

Problem 13.18 [Offset-QPSK]

1. Do the signal-space constellations of QPSK and Offset-QPSK differ?
2. Explain the result in the transmitter scatter plot after pulse shaping.

3. How do the eye patterns in both quadrature components differ?
4. How do the transmitter trajectories of Offset-QPSK and QPSK differ?
5. How do the signals $a_c(t)$, $a_s(t)$, $u_c(t)$, and $u_s(t)$ differ from the respective QPSK signals in Figures 13.60 to 13.63? Note that $a_c(t)$ and $a_s(t)$ can never change simultaneously.

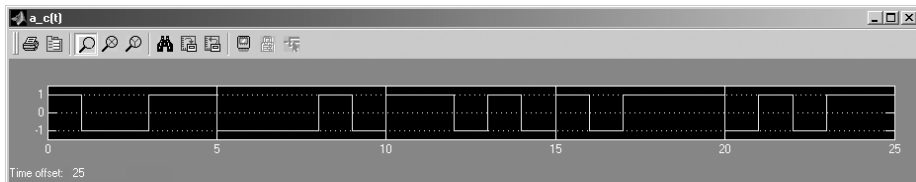


Figure 13.89: In-phase source signal $a_c(t)$

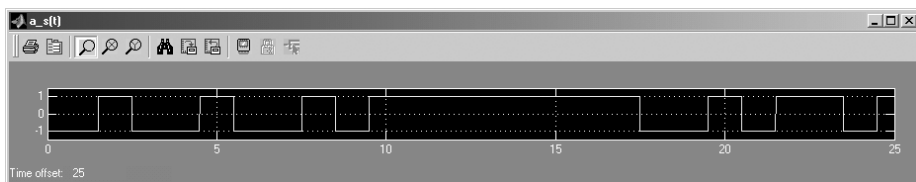


Figure 13.90: Quadrature source signal $a_s(t)$

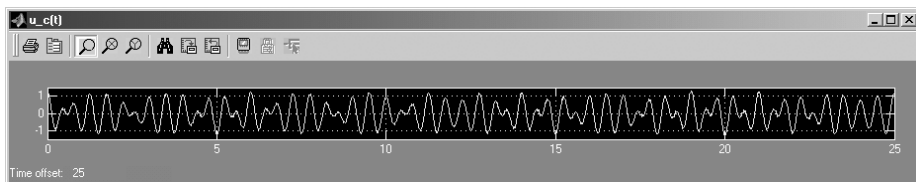


Figure 13.91: In-phase component $u_c(t)$ of the transmitted signal

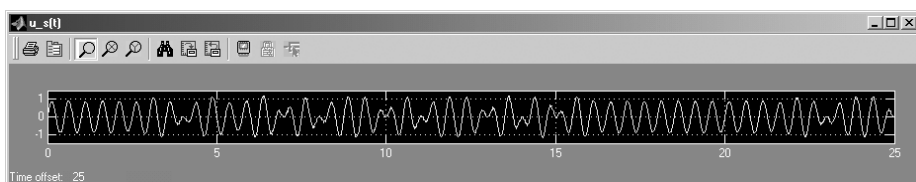


Figure 13.92: Quadrature component $u_s(t)$ of the transmitted signal

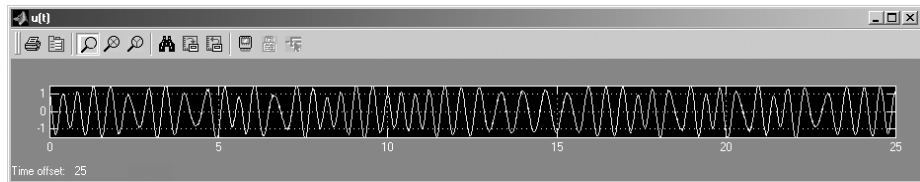
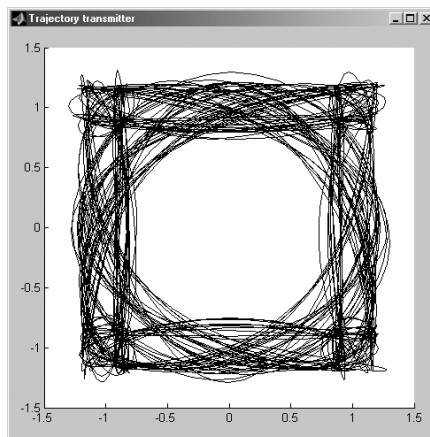
Figure 13.93: Transmitted signal $u(t)$ 

Figure 13.94: Transmitter trajectory for Offset-QPSK

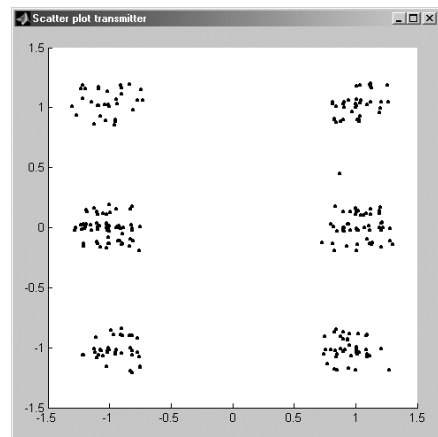


Figure 13.95: Transmitter scatter plot for Offset-QPSK

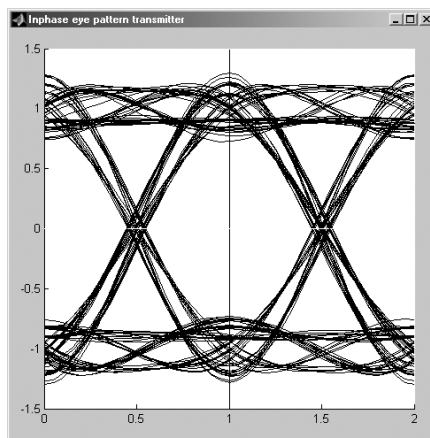


Figure 13.96: Eye pattern in in-phase component at the transmitter for Offset-QPSK

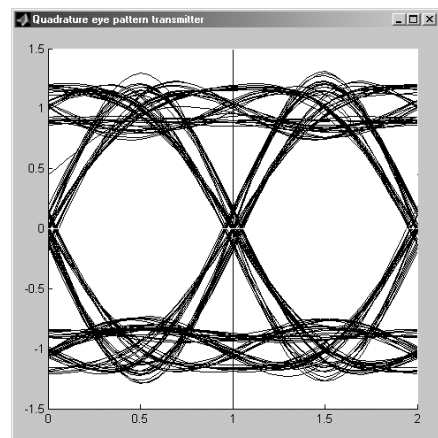


Figure 13.97: Eye pattern in quadrature component at the transmitter for Offset-QPSK

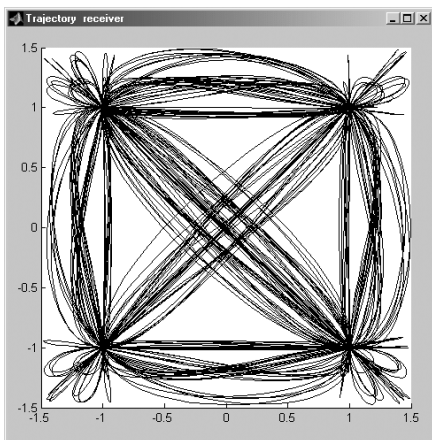


Figure 13.98: Receiver trajectory for Offset-QPSK

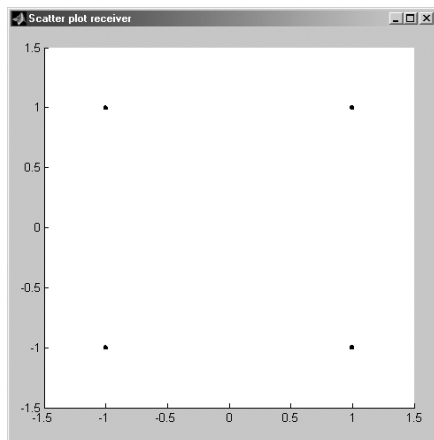


Figure 13.99: Receiver scatter plot for Offset-QPSK

6. Inspect the transmitted signal $u(t)$ and compare the envelope fades with the respective QPSK signal in Figure 13.64. Explain the difference.
7. Why do we observe diagonal transitions in the trajectory at the receiver? Explain using the Simulink receiver model.

SOLUTION

1. No.
2. Due to the delay, the optimum sampling time is shifted by $T/2$ in the quadrature component with respect to the in-phase component. The Simulink scatter plot samples at the optimum sampling time of the in-phase component. Therefore, we observe more than two signal-space clusters in the quadrature component.
3. The eye pattern in the quadrature component is shifted by $T/2$.
4. There are no diagonal transitions for Offset-QPSK.
5. $a_s(t)$ and $u_s(t)$ are shifted by $T/2$ in Offset-QPSK.
6. There are smaller envelopes fades in Offset-QPSK because the data in both quadrature components cannot change simultaneously.
7. The in-phase component is shifted by $T/2$ before the receive filter in order to compensate for the shift of the quadrature component at the transmitter. Therefore we observe the same trajectory as in QPSK.

13.8 Minimum Shift Keying (MSK)

13.8.1 Theory

Binary frequency-shift keying (FSK) was introduced in Section 7.5. We derived the cross-correlation coefficient γ_{mn} between the two signal waveforms as a function of the frequency separation Δf (see Figure 7.25). A frequency separation of $1/2T$ was shown to be the minimum frequency separation for orthogonal signal waveforms. Therefore, binary FSK with $\Delta f = 1/2T$ is called *Minimum Shift Keying (MSK)*.

In general, FSK is a nonlinear digital modulation method. However, due to the orthogonality, MSK can also be viewed as a linear modulation method: MSK is equivalent to Offset-QPSK with cosine pulses and differential precoding. The carrier frequency of the Offset-QPSK is the center frequency

$$f_{c,o} = f_c + \frac{\Delta f}{2} \quad (13.8.1)$$

between the two frequencies $f_1 = f_c$ and $f_2 = f_c + \Delta f$ in the transmitted signal (1.5.2). The Qoffset-QPSK representation of an MSK modulator is depicted in Figure 13.100. The differential precoding is necessary to ensure a continuous phase of the transmitted signal. This is explained in more detail in Proakis and Salehi (2008). Every

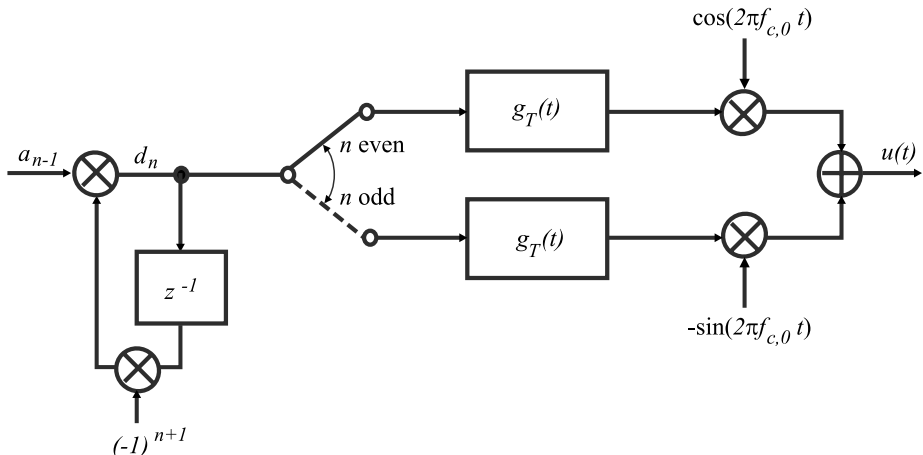


Figure 13.100: Offset-QPSK representation of an MSK modulator

other bit modulates the cos or sin component, respectively. Hence, the delay between both quadrature components is T . Since MSK is a carrier frequency modulation, the envelope of the transmitted signal $u(t)$ is constant. This is achieved by using cosine pulses

$$g_T(t) = \begin{cases} \sqrt{\frac{4E}{T}} \cos\left(\frac{\pi t}{2T}\right) & -T \leq t \leq T \\ 0, & \text{otherwise} \end{cases} \quad (13.8.2)$$

13.8.2 Experiments

Choose *MSK* from the main menu and start the simulation. The basic Simulink model is similar to the QPSK model depicted in Figure 13.57. The MSK transmitter model is depicted in Figure 13.101. Figures 13.102 to 13.112 show the MSK diagrams.

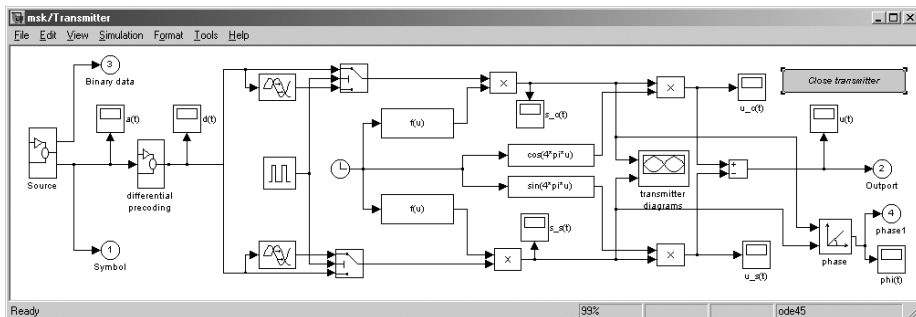


Figure 13.101: Simulink model for MSK transmitter

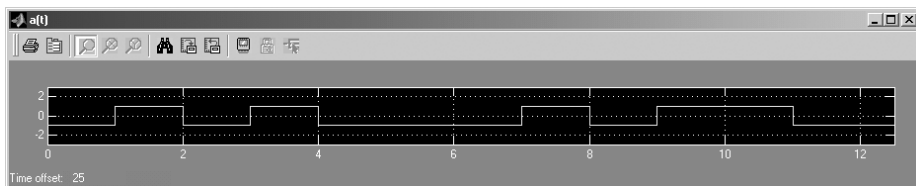


Figure 13.102: Source signal $a(t)$

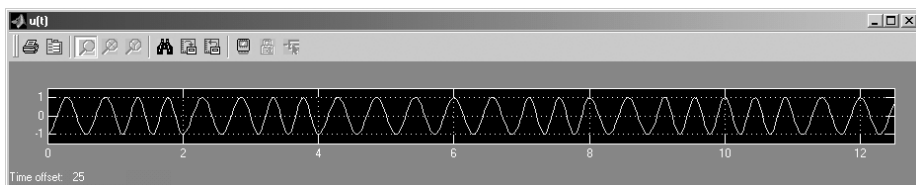


Figure 13.103: Transmitted signal $u(t)$

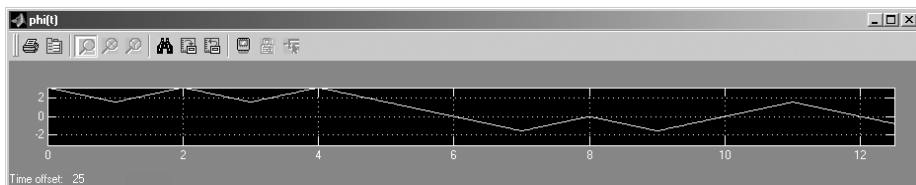
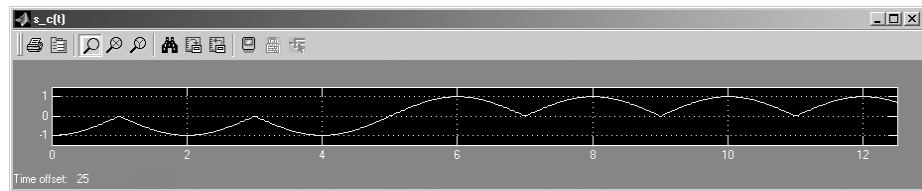
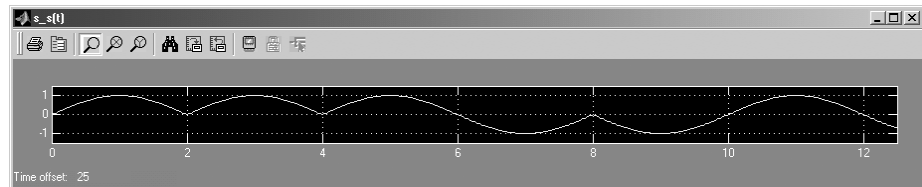
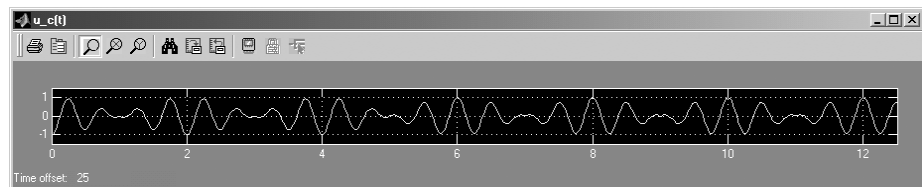
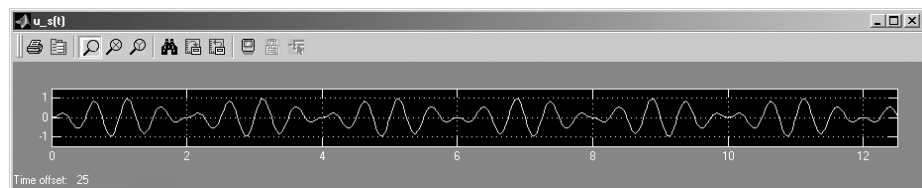


Figure 13.104: Phase of trajectory

Figure 13.105: In-phase baseband signal $s_c(t)$ Figure 13.106: Quadrature baseband signal $s_s(t)$ Figure 13.107: In-phase component $u_c(t)$ of the transmitted signalFigure 13.108: Quadrature component $u_s(t)$ of the transmitted signal

TUTORIAL PROBLEM

Problem 13.19 [Binary Frequency Shift Keying] Place the window of the source signal $a(t)$ above the window of the transmitted signal $u(t)$.

1. Observe that MSK is a frequency modulation, i.e., the information is contained in the carrier frequency and the envelope of the transmitted signal $u(t)$ is constant.
2. How does a constant envelope show up in the trajectory?

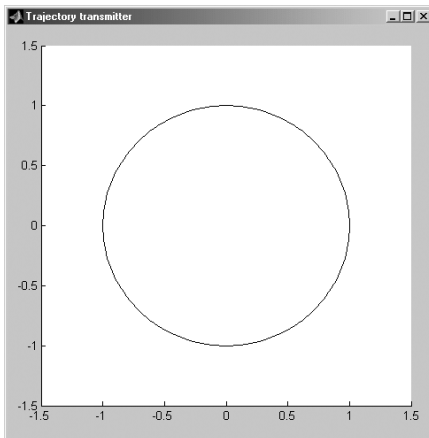


Figure 13.109: Transmitter trajectory for MSK

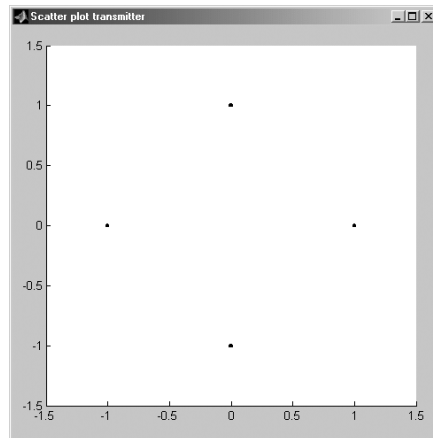


Figure 13.110: Transmitter scatter plot for MSK

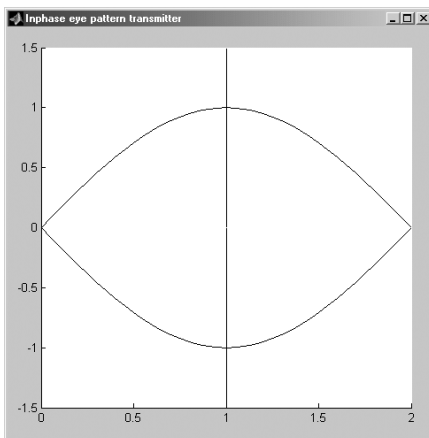


Figure 13.111: Eye pattern in in-phase component at the transmitter for MSK

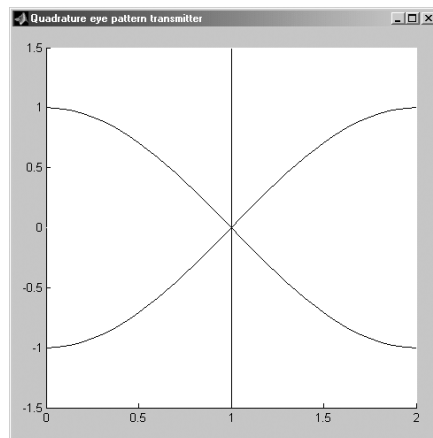


Figure 13.112: Eye pattern in quadrature component at the transmitter for MSK

SOLUTION

1. For $a(t) = 1$ the carrier frequency is higher than for $a(t) = -1$. However, since the minimum frequency spacing for orthogonal signals is chosen, the difference in frequency is not easy to see.
2. The trajectory is a circle.

Drag the trajectory window to the middle of the screen so that it is not concealed by other windows after a restart of the simulation. Restart the simulation and observe the trajectory.

TUTORIAL PROBLEM

Problem 13.20 [Minimum Shift Keying]

1. Explain the behavior of the trajectory taking into account the source signal $a(t)$. (The trajectory is displayed starting with the second source bit.)
2. Observe the phase $\phi(t)$ of the trajectory and compare it with the source signal $a(t)$. What is the phase shift during a period of T ? Note the continuous phase, which is obtained due to differential precoding.

SOLUTION

1. The trajectory rotates on a circle by $\pm\pi/2$ per T . This follows with the MSK frequency separation $\Delta f = 1/2T$ and (13.8.1) from the transmitted signal according to (1.5.2):

$$\begin{aligned} u_m(t) &= \sqrt{\frac{2E}{T}} \cos(2\pi f_c t + 2\pi m \Delta f t) \\ &= \sqrt{\frac{2E}{T}} \cos(2\pi f_{c,o} t + 2\pi(1-2m) \frac{\Delta f}{2} t) \\ &= \sqrt{\frac{2E}{T}} \cos(2\pi f_{c,o} t + \pi(1-2m) \frac{t}{2T}) \end{aligned}$$

2. The phase changes linearly by $\pm\pi/2$ per T .

We now examine how MSK can be represented as Offset-QPSK. Double-click on the blue box *Transmitter* to open the Simulink transmitter model depicted in Figure 13.101.

Observe the baseband signals $s_c(t)$ and $s_s(t)$ in both quadrature components after pulse shaping. The cos pulses ensure that the transmitted signal $u(t)$ has constant envelope or equivalently that the trajectory is a circle.

TUTORIAL PROBLEM

Problem 13.21 [Offset-QPSK Representation of MSK]

1. What is the temporal spacing of the cos pulses in the quadrature components and the delay of the quadrature component with respect to the in-phase component?
2. Explain why four points occur in the transmitter scatter plot.

SOLUTION

1. Spacing: $2T$; delay of quadrature component: T .

2. The trajectory is sampled at rate $1/T$. From Figures 13.105 and 13.106 it can be seen that $s_c(2kT) = \pm 1$ and $s_s(2kT) = 0$, whereas $s_c((2k+1)T) = 0$ and $s_s((2k+1)T) = \pm 1$. Therefore, sampling the trajectory at $2kT$ yields an in-phase point in the scatter plot, whereas sampling at $(2k+1)T$ yields a quadrature point.

MSK can be coherently demodulated in the same way as Offset-QPSK followed by a differential decoder. Therefore, we do not have to deal with demodulation explicitly here.

13.9 16-ary Quadrature Amplitude-Shift Keying (16-QAM)

13.9.1 16-QAM with Square-Root Raised-Cosine Pulses

Examine 16-QAM with square-root raised-cosine pulses:

16-QAM > Root-RC

The Simulink model and the transmitter model are depicted in Figures 13.113 and 13.114. In 16-QAM, $b = 4$ bits are mapped on a signal-space constellation point.

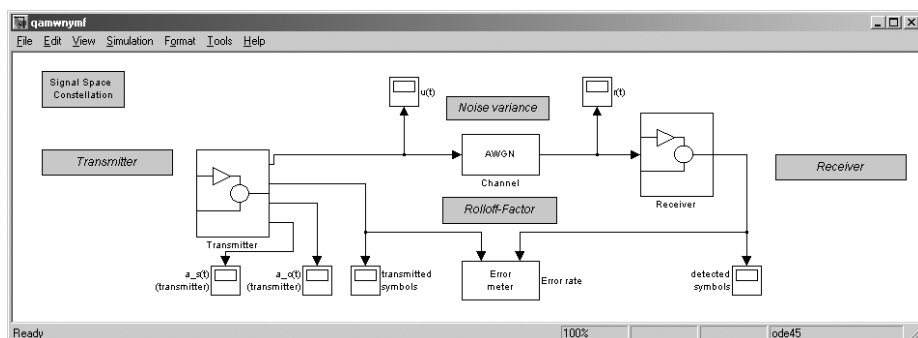


Figure 13.113: Simulink model for 16-QAM with square-root RC pulses

You can view the signal-space constellation in Figure 13.115 by double-clicking on the blue box *signal-space Constellation*.

TUTORIAL PROBLEM

Problem 13.22 [Gray Mapping] Check if the labeling is done according to a Gray mapping, i.e., constellation points with minimum Euclidean distance differ in only one bit. What is the purpose of using Gray mapping instead of an arbitrary mapping of bits to constellation points? Is Gray mapping possible for higher-order QAM modulation?

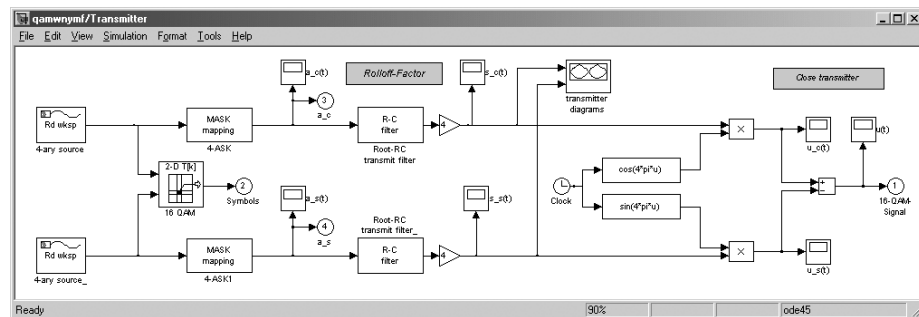


Figure 13.114: Simulink model for 16-QAM transmitter with square-root RC pulses

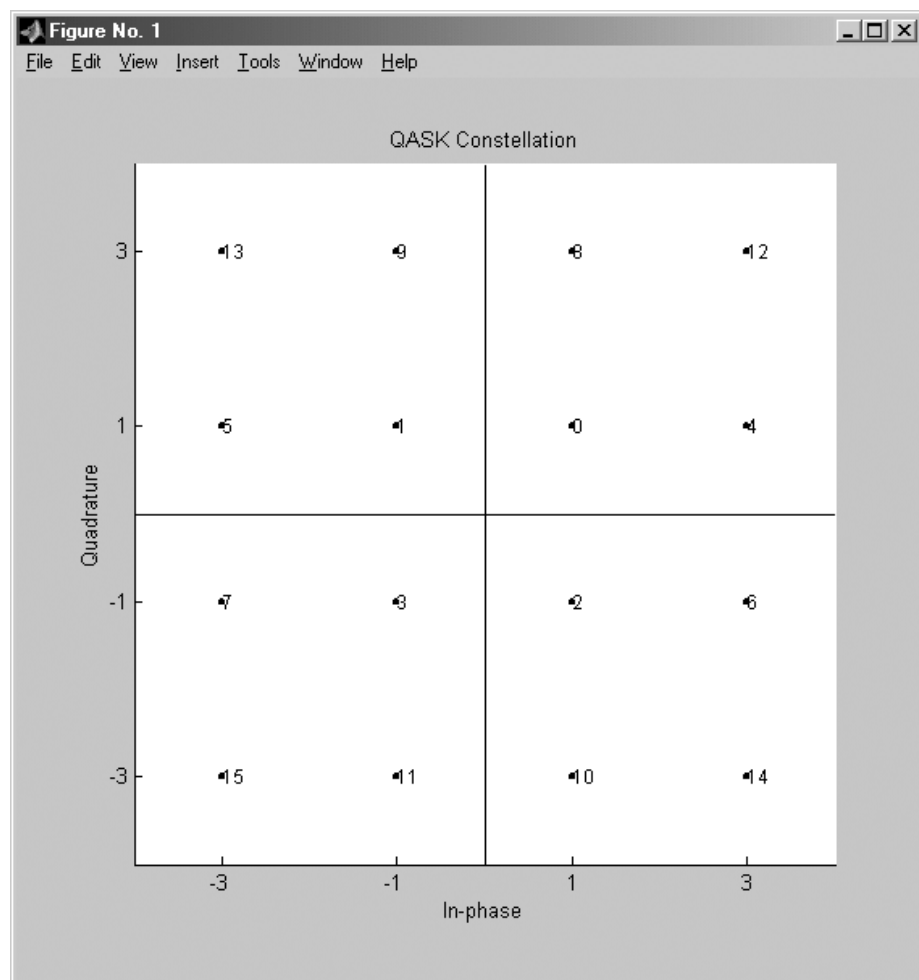


Figure 13.115: 16-QAM signal-space constellation

SOLUTION

The binary representation of the decimal numbers yields a Gray mapping. The most likely error event for sufficiently high SNR is detecting a constellation point with minimum Euclidean distance to the actually transmitted constellation point. With Gray mapping this error event results in only one bit error. Assigning a single bit error to the more likely error events and multiple bit errors to less likely error events minimizes the average bit error probability. A Gray mapping can also be found for higher-order QAM.

Start the simulation. Since the signals in the quadrature component look like the respective in-phase signals, only the in-phase signals are depicted in Figures 13.116 to 13.125 for noiseless transmission. For noisy transmission the receiver scatter plot looks similar to Figure 13.121.

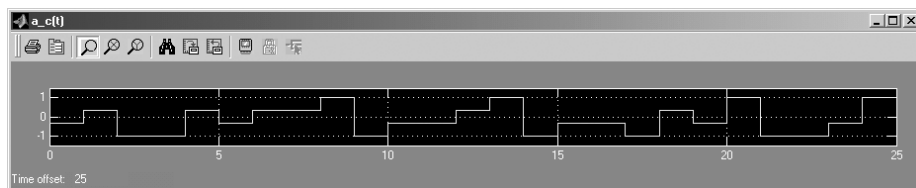


Figure 13.116: In-phase source signal $a_c(t)$

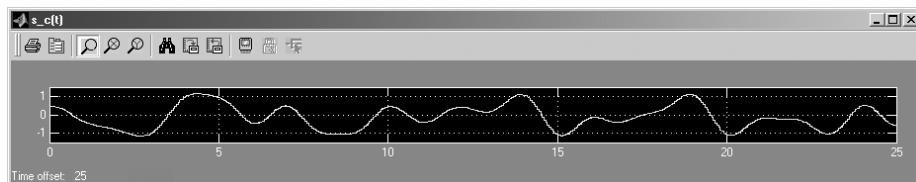


Figure 13.117: In-phase baseband signal $s_c(t)$

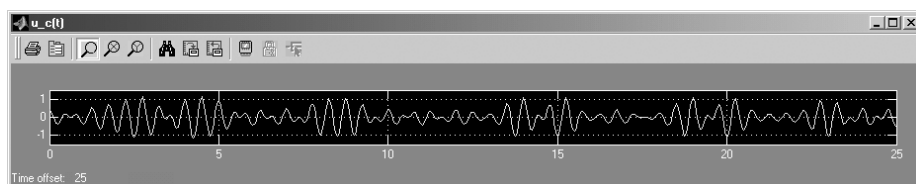


Figure 13.118: In-phase component $u_c(t)$ of the transmitted signal

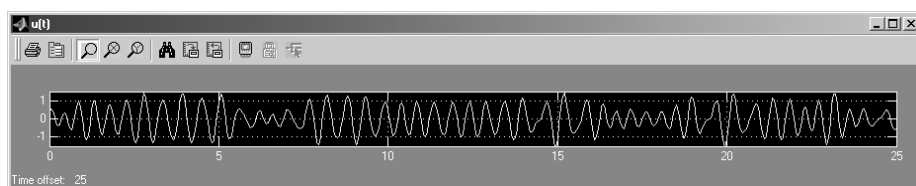


Figure 13.119: Transmitted signal $u(t)$

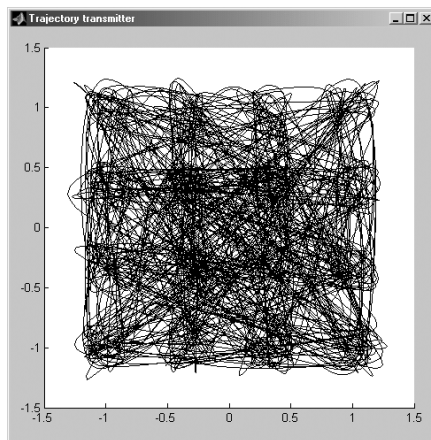


Figure 13.120: Transmitter trajectory for 16-QAM with square-root raised-cosine pulses

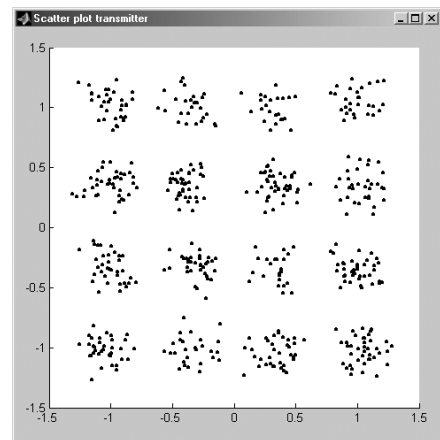


Figure 13.121: Transmitter scatter plot for 16-QAM with square-root raised-cosine pulses

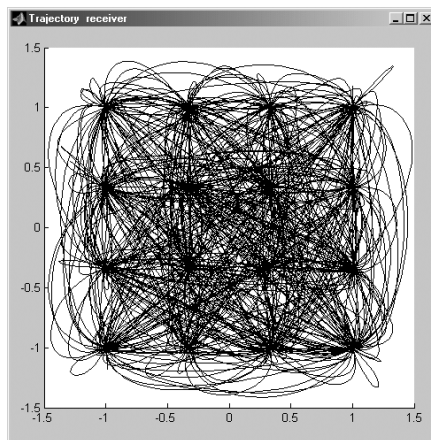


Figure 13.122: Receiver trajectory for 16-QAM with square-root raised-cosine pulses

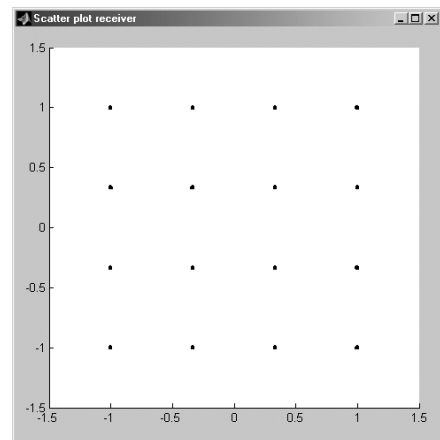


Figure 13.123: Receiver scatter plot for 16-QAM with square-root raised-cosine pulses

TUTORIAL PROBLEM

Problem 13.23 [Sensitivity to Additive Noise] Is 16-QAM more or less sensitive to additive noise than QPSK? Explain using the eye patterns and the signal-space constellation.

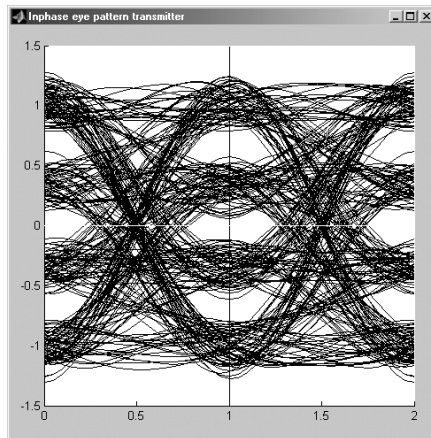


Figure 13.124: Eye pattern in in-phase component at the transmitter for 16-QAM with square-root raised-cosine pulses

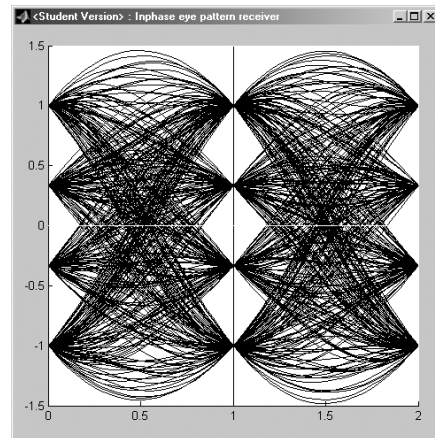


Figure 13.125: Eye pattern in in-phase component at the receiver for 16-QAM with square-root raised-cosine pulses

SOLUTION

16-QAM is more sensitive to additive noise since for the same per symbol energy the minimum Euclidean distance of the constellation points is smaller. We observe four nodes in the eye patterns, which results in a smaller vertical eye opening and higher sensitivity to additive noise.

13.9.2 16-QAM with Raised-Cosine Pulses

We now replace the square-root raised-cosine pulses by raised-cosine pulses:

16-QAM > Raised-Cosine

The relevant diagrams are depicted in Figures 13.126 to 13.129.

TUTORIAL PROBLEM

Problem 13.24 [16-QAM with Raised-Cosine Pulses ($\alpha = 0.5$)] Do errors occur if no noise is present? Explain, using the eye patterns and scatter plot at the receiver.

SOLUTION

Using a raised-cosine transmit filter and a matched filter at the receiver results in ISI. Due to the small minimum Euclidean distance of the signal-space constellation points, the ISI imposed by wrong filter design causes errors even if no noise is present. In the eye patterns it can be observed that error-free detection is not possible.

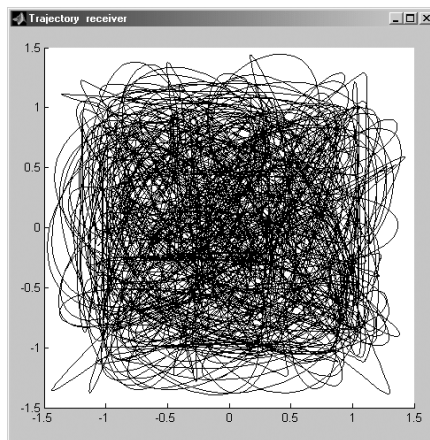


Figure 13.126: Receiver trajectory for 16-QAM with raised-cosine pulses ($\alpha = 0.5$)

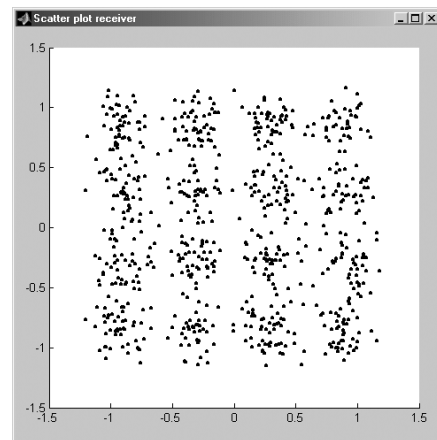


Figure 13.127: Receiver scatter plot for 16-QAM with raised-cosine pulses($\alpha = 0.5$)

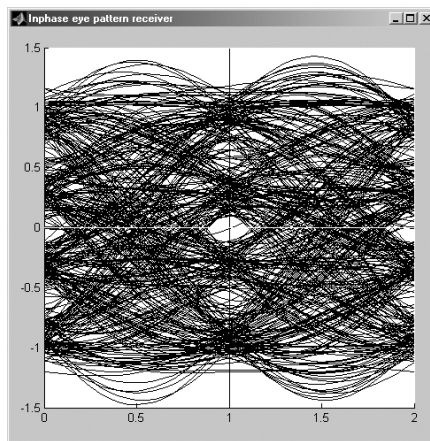


Figure 13.128: Eye pattern in in-phase component at the receiver for 16-QAM with raised-cosine pulses ($\alpha = 0.5$)

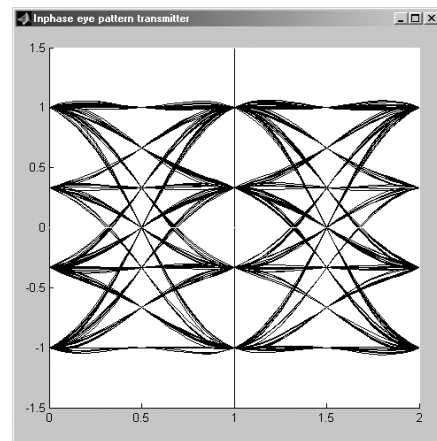


Figure 13.129: Eye pattern in in-phase component at the transmitter for 16-QAM with raised-cosine pulses ($\alpha = 1$)

Set the rolloff factor of transmit and receive filter to $\alpha = 0.1$ and later to $\alpha = 1$ using the scrollbar, which is opened by a double-click on the blue box *Roll-off factor*.

TUTORIAL PROBLEM

Problem 13.25 [16-QAM with Raised-Cosine Pulses ($\alpha \neq 0.5$)]

1. Do more or less errors occur than for $\alpha = 0.5$ if no noise is present?

2. Why do we observe nodes at $t = 0.5T$ and $t = 1.5T$ in the eye patterns at the transmitter for $\alpha = 1$? To solve this problem you can go back to *Pulse Shape* in the main menu.

SOLUTION

1. For $\alpha = 0$, raised-cosine and square-root raised-cosine pulses are identical and there is zero ISI at the receiver. Therefore, for small rolloff factors $\alpha \rightarrow 0$, the BER due to ISI decreases compared to $\alpha = 0.5$. For large rolloff factors, the impulse response decreases quite fast. However, the ISI to the next neighbor is relatively strong. This can be observed from the convolution of two raised-cosine pulses as displayed from the menu *Pulse Shape > Convolution* and depicted in Figure 13.22. Therefore, for large rolloff factors $\alpha \rightarrow 1$, the BER is higher than for $\alpha = 0.5$.
2. For raised-cosine-pulses with $\alpha = 1$, we have:

$$g_T\left(\frac{kT}{2}\right) = \begin{cases} 1, & k = 0 \\ \frac{1}{2}, & k = \pm 1 \\ 0, & \text{otherwise} \end{cases}$$

Therefore, we observe nodes in the eye pattern at $\frac{2k+1}{2}T$.

Problems

13.1 Show that additive white Gaussian noise remains white after sampling if a square-root raised-cosine receive filter is used.

13.2 BPSK requires estimation of the carrier phase at the receiver. Show analytically what is the effect of a carrier-phase offset φ , i.e., demodulation with $2 \cos(2\pi f_c t + \varphi)$.

13.3 In Section 1.3.2 differential phase-shift keying was introduced as a method to enable detection without carrier-phase estimation. Build a Simulink model for binary differential phase-shift keying with NRZ rectangular pulses based on the BPSK model in Figure 13.2. Observe if error-free detection is possible in the case of carrier-phase offset.

13.4 Derive the effect of a carrier-phase-offset φ analytically in a QPSK system.

13.5 Derive the effect of a carrier-frequency-offset Δf analytically in a QPSK system.

13.6 Another method to avoid diagonal transitions of the trajectory through the origin is differential $\pi/4$ -QPSK. The information is coded in the phase difference of successive symbols according to

$$\varphi_k = \varphi_{k+1} + \Delta\varphi_m$$

where k is the time index and

$$\Delta\varphi_m = \frac{\pi}{2}m + \frac{\pi}{4}$$

where $m = 0, 1, 2, 3$ is the index of the transmit symbol. Show by an example that every other symbol is taken from a QPSK constellation that is phase-shifted by $\pi/4$ relative to the QPSK constellation of the previous symbol and therefore, transitions through the origin are avoided.

13.7 According to Figure 1.28 we obtain orthogonal signal waveforms for FSK if the frequency separation between the two signal waveforms is a multiple of $1/(2T)$. What is the advantage of choosing a frequency separation of $1/(2T)$?

13.8 Show that Offset-QPSK with cosine pulses according to (13.8.2) has a constant envelope. Assume a delay of T between in-phase and quadrature component as in the Offset-QPSK representation of MSK.

13.9 Show that for NRZ rectangular pulses, an integrate and dump receiver yields the same output samples as a rectangular NRZ receive filter, i.e. the matched filter can be implemented as integrate and dump.

13.10 What is the design criterion for the receive filter which yields the matched filter solution?

13.11 Assume a transmission system with causal square-root raised-cosine pulse shaping and a matched filter receiver. Both the impulse responses of transmit and the receive

filter are limited in time to a duration of $12T$. Determine the overall delay of the transmission system. Verify your solution in the respective Simulink model.

13.12 Derive the bit error probability for QPSK with Gray mapping and for QPSK with natural mapping. Create a Simulink model and try to verify the analytical results via simulation.

13.13 It can be shown that the symbol error probability of M -PSK for $E/N_0 \gg 1$ —the so-called asymptotic symbol error probability—can be approximated by

$$P_e \approx 2Q\left(\sqrt{\frac{d_{min}^2 E}{2N_0}}\right).$$

Here

$$d = |s_1 - s_2| \quad (s_1 \text{ and } s_2 \text{ are signal constellation points})$$

denotes the Euclidian distance between two signal constellation points on the unit circle and d_{min} is the minimum Euclidean distance between two points of the constellation. Give the asymptotic difference of the SNR E/N_0 in dB between the curves of the symbol error for 2-, 4- and 8-PSK, respectively! How do the curves change if plotted versus the SNR E_b/N_0 per transmitted information bit? Create a Simulink model and try to verify the analytical results via simulation.

13.14 Consider QAM with the following signal-space constellation points:

$$s_m \in \{\pm 1 \pm j, \pm 2 \pm j2, \pm 1 \pm j2, \pm 2 \pm j1\}.$$

1. Sketch the signal-space constellation. What can you observe?
2. How many information bits can be transmitted in one symbol?
3. The transmitted bits are often of different significance. For example, if we transmit sampled values then the sign bit is of greater importance than the least significant bit (LSB). Hence, it is efficient to protect the bits unequally against transmission errors. Determine a mapping rule for information bits to symbols such that the first two bits of each symbol are better protected than the following bits. Add the result to your signal constellation plot of (a).
4. Calculate the average energy E per symbol for equally likely information bits. For pulse shaping, we use a rectangular pulse with amplitude A (during the whole symbol duration).